Title ***Article: Discoveries***

Diurnality shapes the visual opsin genes of colorful Neotropical frogs

Running title

Opsin gene evolution in diurnal and colorful frogs

Authors

Wan, YC[1,2,†], MJ Navarrete[1,3,†], LA O'Connell[4], LH Uricchio[1], A Roland[4,5], ME Maan[6], SR Ron[3], M Betancourth-Cundar[7], MR Pie[8,9], KA Howell[10], CL Richards-Zawacki[10], ME Cummings[11], DC Cannatella[11,12], and JC Santos[13,*], RD Tarvin[1,*]

[1] Museum of Vertebrate Zoology and Department of Integrative Biology, University of California Berkeley, Berkeley, CA, USA 94720

[2] School of Biomolecular and Biomedical Science, University College Dublin, Belfield, Dublin, Ireland

[3] Museo de Zoología, Facultad de Ciencias Exactas y Naturales, Pontificia Universidad Católica del Ecuador, Quito, Ecuador

[4] Department of Biology, Stanford University, Palo Alto, CA, USA 94305

[5] Research Centre on Animal Cognition (CRCA), Centre for Integrative Biology (CBI), UMR5169 CNRS, Toulouse University, Toulouse, France

[6] Groningen Institute for Evolutionary Life Sciences, University of Groningen, Nijenborgh 7, 9747 AG Groningen, The Netherlands

[7] Departamento de Ciencias Biológicas, Universidad de los Andes, Bogotá, Colombia, 111711

[8] Department of Zoology, Universidade Federal do Paraná, Curitiba, Brazil, 81531-980

[9] Biology Department, Edge Hill University, Ormskirk, UK L39 4QP

[10] Department of Biological Sciences, University of Pittsburgh, Pittsburgh, PA, USA 15260

[11] Department of Integrative Biology, University of Texas at Austin, Austin, TX, USA 78712

[12] Biodiversity Center, University of Texas at Austin, Austin, TX, USA 78712

[13] Department of Biological Sciences, St John's University, NY, USA 11439

* Corresponding Authors

[†] YCW and MJN contributed equally as first authors and agree that each has the right to list themselves as first author on their CVs.

Corresponding authors

* RD Tarvin, rdtarvin@berkeley.edu (510) 642-0308

* JC Santos, santosj@stjohns.edu (718) 990-1656

Author contributions

RDT and JCS conceptualized the study; YCW, JCS, LHU, RDT, LAO, MJN, AR, MEC collected data; YCW, JCS, LHU, RDT performed analyses; DCC, LAO, RDT, MEC, and JCS acquired funding; RDT, JCS, MBC, MEM conducted fieldwork; MRP, MEC, MEM, CLR-Z, SRR, MBC, RDT, and JCS contributed samples and helped with permits; YCW, MJN, LHU, JCS, LH, and RDT prepared the original draft; RDT coordinated the project; RDT and JCS supervised the study; all authors reviewed and revised the manuscript.

Acknowledgments

This research was funded by NSF DEB-1556967 to DCC; NSF GROW, NSF DDIG (DEB-1404409), National Geographic Society 2014 Young Explorer Grant, and UC Berkeley start-up funding to RDT; NIH 5P50GM068763, NSF IOS-1822025 and William F. Milton Fund from Harvard Medical School to LAO; LAO is a New York Stem Cell Foundation – Robertson Investigator. JCS was supported by SJU start-up funds and NSF DEB-2016372. MJN was supported by the American Association of University Women (AAUW). We thank Roberto Ibañez and Brian Gratwicke (Amphibian Rescue and Conservation Project), Luis A. Coloma (Fundación Otonga and Centro Jambatu de Investigación y Conservación de Anfibios; Quito, Ecuador), Adolfo Amézquita (Laboratory of Biodiversity and Cloud Forests Conservancy, Bioconservancy; Jardín, Colombia), César Aguilar (Universidad Nacional Mayor de San Marcos; Lima, Peru), and Travis LaDuc (Biodiversity Center, UT Austin) for facilitating access to tissues and specimens.

Data accessibility statement

Raw Illumina sequencing data are deposited in the Sequence Read Archive (BioProject PRJNA856227). Specimens are available in QCAZ at Pontificia Universidad Católica del Ecuador, Centro Jambatu de Investigación y Conservación de Anfibios (Quito, Ecuador), Museo de Historia Natural de la Universidad Nacional Mayor de San Marcos (MUSM, Lima, Peru), Coleção de Herpetologia, Departamento de Zoologia, Universidade Federal do Paraná, (Paraná, Brazil), or Museo de Historia Natural ANDES at the Universidad de los Andes. All scripts and other data are available in the supporting material.

Conflict of Interest: This publication is based in part on work by DCC while serving at the National Science Foundation. Any opinion, findings, and conclusions or recommendations expressed in this material are those of the author(s) and do not necessarily reflect the views of the National Science Foundation or United States government.

Title

Diurnality shapes the visual capacity of colorful Neotropical frogs

Abstract

Amphibians are an ideal model for studying visual system evolution because their biphasic (aquatic and terrestrial) life history and ecological diversity expose them to a broad range of visual conditions. Here we evaluate signatures of selection on visual opsin genes of five Neotropical diurnal frog groups, with a focus on three conspicuously colored and chemically defended (i.e., aposematic) clades: poison frogs (Dendrobatidae), Harlequin toads (Bufonidae: *Atelopus*), and pumpkin toadlets (Brachycephalidae: *Brachycephalus*). We found evidence of positive selection on 15 amino acid sites in *LWS*, *SWS1*, *SWS2*, and *RH1* opsin genes, of which one in *LWS* has been previously identified as important for spectral tuning in other vertebrates. Patterns of selection reveal that the evolution of diurnality was important in shaping the vision of focal frog groups; whether conspicuous coloration has played a role remains unclear, as no support was found but inferences may have been statistically limited by sample size. Furthermore, we provide evidence that the *SWS2* gene, normally expressed in rod cells in amphibians, has likely been lost in the ancestor of Dendrobatidae, suggesting that under low light levels, dendrobatids have inferior wavelength discrimination compared to other frogs. This might coincide with the diurnal activity of dendrobatids and could have implications for opsin evolution in this clade. Our analyses show that studies of opsin diversification could expand our understanding of how adaptations for diel habits evolve and how visual tuning alters the sensory landscape of animals.

Keywords: Gene loss, vision, blue-sensitive opsin, *Atelopus*, *Brachycephalus*, aposematism

Introduction

Natural selection has favored visual systems that maximize the detection and discrimination of light wavelengths that are relevant to organismal activity patterns (Warrant and Johnsen 2013). For instance, nocturnal species have visual systems that capture maximal light in dim lighting conditions (Cronin et al. 2014) while crepuscular species, which are mostly active during twilight hours, have enhanced color discrimination in low-light conditions (Mohun and Davies 2019). In contrast, diurnal species are active when the light spectrum is the brightest and broadest (e.g., 350-700 nm); therefore, their visual systems may be evolutionarily tuned for improved wavelength discrimination (i.e., better color vision) (Mohun and Davies 2019). Vision in anuran amphibians is particularly interesting as the visual system often needs to transition from functioning in an aquatic environment during the larval stage to a terrestrial environment during the juvenile phase. Each setting presents unique visual requirements (Cronin et al. 2014). Furthermore, while most frogs are primarily nocturnal or crepuscular, a few clades

have evolved diurnal activity (Anderson and Wiens 2017). Many of these diurnal frogs are adorned with colorful visual signals that evolved as part of a defensive strategy known as aposematism, in which conspicuous signals warn predators of prey defenses (Santos et al. 2003; Tarvin et al. 2017). Although aposematic signals initially evolve under selective pressure from predators (Mappes et al. 2005; Sherratt 2008), warning signals can become subject to sexual selection (Cummings and Crothers 2013; Rojas et al. 2018) – that is, if the intended observer's sensory system is appropriately tuned to the signal.

Vision in vertebrates relies on a set of photosensitive opsin genes that encode diverse G-protein-coupled receptors that bind to a retinal chromophore (Bowmaker 2008). The visual opsin genes present in vertebrates include long-wavelength sensitive (*LWS* or *OPN1LW*), middle-wavelength sensitive (*RH2*, *MWS* or *RHB*; not to be confused with an independent gene duplication that gave rise to a middle-wavelength-sensitive opsin gene in Old World primates also called *MWS*, or *OPN1MW* [Nathans et al. 1986; Hunt et al. 1998]), short-wavelength sensitive 1 (*SWS1* or *OPN1SW*), and short-wavelength sensitive 2 (*SWS2* or *OPN2SW*; Bowmaker 2008; Schott et al. 2022). The gene encoding the rod opsin, rhodopsin (*RH1*, *RHO*, *RHA*, or *OPN2*), evolved after a duplication and divergence event from an ancestral opsin shared with *RH2* (Okano et al. 1992). Color vision is achieved when two or more photoreceptors with opsins differing in wavelength sensitivity are simultaneously activated and their signals are compared by the observer's central nervous system (Bowmaker 2008). For consistency, we refer to the opsin genes using the following acronyms: *LWS*, *SWS1*, *SWS1*, *RH1*, *RH2*.

The anuran retina is thought to typically contain two types of cone cells that are active under bright-light conditions: "double cones", which express two copies of the *LWS* opsin, and "single cones", which express *SWS1* (Liebman and Entine 1968; Koskelainen et al. 1994; Mohun and Davies 2019; Donner and Yovanovich 2020). Some anuran species such as *Rana pipiens* (nocturnal) and *Oophaga pumilio* (diurnal), possess a third middle-wavelength-sensitive cone (λ_{max} of ~500 nm), but the pigment contained in this type of photoreceptor cells remains unknown (Siddiqi et al. 2004; Mohun and Davies 2019). In some vertebrates (e.g., fish and reptiles; Bowmaker 2008), the *RH2* gene is responsible for green or middle-wavelength-sensitivity. However, the *RH2* gene has not been found in any amphibian to date and is believed to have been lost in an ancestor of amphibians (Mohun and Davies 2019; Schott et al. 2022). Thus, it is plausible that *RH1* is the gene that is expressed in green-sensitive cones, conferring amphibians the ability to detect middle-wavelength light spectra during the day, as has occurred in at least one species of snake (Schott et al. 2016). In addition to these three cone cell types, the anuran retina has two types of rod cells that are active in dim-light conditions: one that expresses *RH1*, known as the "red rod", and another that expresses *SWS2*, known as the "green rod" (Hunt and Collin 2014). The second rod type likely allows some amphibians to have low-light (scotopic) and rod-based color discrimination, but this has not been empirically tested (Yovanovich et al. 2017). Although some vertebrates use oil droplets to further tune wavelength sensitivity, oil droplets in anurans (including in *O. pumilio*) are often absent or

colorless and thus are unlikely to influence the spectral sensitivity of cone opsin proteins (Siddiqi et al. 2004; Toomey and Corbo 2017).

While a few anuran models (e.g., *Rana temporaria, Xenopus laevis,* and *Rhinella marina* [*Bufo marinus*]) have played critical roles in discovering the biology of vision, none of these species are diurnal; the diversity of anuran visual systems is only just beginning to be unraveled (Donner and Yovanovich 2020). For example, lens transmission properties (Yovanovich et al. 2020; Thomas et al. 2022) have been measured for only 108 of the >7500 currently described anuran taxa (AmphibiaWeb 2022) and spectral sensitivity of retinal photoreceptor cells is described for only 10 species (Donner and Yovanovich 2020). The genetic basis of anuran vision is especially understudied (Mohun and Davies 2019), with genomic resources until very recently limited to only a handful of well-annotated frog genomes (Womack et al. 2022) and one recent ecological study of opsin genes in 33 frogs (Schott et al. 2022).

The lack of information regarding the diversification of anuran vision contrasts with the relatively large body of research into their array of visual signals (e.g., Toledo and Haddad 2009; Bell and Zamudio 2012; Rößler et al. 2019; Yeager and Barnett 2021). Intensive research efforts over recent decades have turned dendrobatid frogs into a model system for understanding how natural selection by predators shapes the origin and subsequent diversification of aposematic signals (e.g., Clough and Summers 2000; Wollenberg et al. 2008; Richards-Zawacki and Cummings 2011; Santos and Cannatella 2011; Wang 2011; Cummings and Crothers 2013; Rojas et al. 2014; Lawrence et al. 2019). The role of dendrobatid warning signals in intraspecific communication is less studied, but color is important for mate recognition and territorial displays in some dendrobatid species. For example, in the aposematic species *O. pumilio,* tadpoles imprint on their mother's color (Yang et al. 2019), females show assortative mate preferences (Summers et al. 1999; Reynolds and Fitzpatrick 2007; Maan and Cummings 2008; Yang et al. 2016), male-male competition relies on color-mediated aggressive behaviors towards phenotypically similar rivals (Yang et al. 2018; Yang and Richards-Zawacki 2020), and there may be directional sexual selection on male coloration brightness (Maan and Cummings 2009). Assortative mating by coloration and pattern is present but less pronounced in other species of the same genus (*O. histrionica* and *O. lehmanni*) (Medina et al. 2013). In contrast, there is little evidence for color-based intraspecific signaling in the brightly colored species of *Atelopus* (Harlequin toads, Bufonidae) and *Brachycephalus* (Pumpkin toadlets, Brachycephalidae). Nevertheless, at least one species of *Brachycephalus* is inferred to be aposematic based on experimental evidence (Rebouças et al. 2019), and some species of *Atelopus* have conspicuously colored soles that might be aposematic signals (Rößler et al. 2019). While territorial males of some species from both genera display a foot-waving behavior to warn off encroaching males (Pombal et al. 1994), it is unclear how important a role color and/or contrast play in this display. Likewise, there have not been any studies examining color-based mate preference in these genera.

Here we evaluated two hypotheses regarding vision in anuran species: 1) if the transition to diurnality is a major driver of opsin evolution in anurans, then we expected to detect positive selection on amino acids at or near spectral tuning sites in opsins of diurnal frog species; and 2) if conspicuous warning signals (i.e., bright coloration) are important for sexual communication in aposematic frogs, then we expected to detect additional patterns of positive selection on amino acids at or near spectral tuning sites in opsins of colorful frog clades. We sequenced the four amphibian visual opsin genes known in amphibians (*LWS*, *SWS1*, *SWS2* and *RH1*) from 116 species representing Neotropical frog clades with five independent origins of conspicuous coloration. The wavelength sensitivity of opsin proteins can be modified by natural selection via changes in the amino acid sequence to better absorb wavelengths that are most relevant to the organism, a process known as spectral tuning (Carvalho et al. 2007; Hunt et al. 2007; Osorio and Vorobyev 2008). Using a combination of site and branch-site selection analyses, we determined whether amino acid positions at or near known spectral tuning sites were under selection. Additionally, we aimed to determine whether poison frogs had lost *SWS2* using transcriptome sequencing, exome capture, and genome canvassing. Finally, we propose a potential role for *RH1* in the middle-wavelength-sensitive cone cell found in some amphibians including dendrobatids.

Results

Opsin sequences. We retrieved 28 opsin gene sequences of 13 species from GenBank and reconstructed another 49 (representing 19 species) using SRA data deposited in NCBI (Table S1). From 484,530 Illumina reads from our bait capture experiment, we further reconstructed 289 new opsin gene sequences representing 87 anuran species. In total we analyzed 366 sequences from 116 anuran species. Raw reads are available in the Sequence Read Archive (PRJNA856227); assembled sequences are available on DataDryad (DOI: TBD). All assembled sequences had an average read coverage of >10x, with 82% having coverage >50x (Table S2).

Analyses of selection. HyPhy site and branch-site selection tests identified a total of 15 sites across the four opsin genes as having experienced pervasive (FEL) or episodic (MEME) positive selection in diurnal (D) or diurnal and brightly colored (DC) frogs (Table 1). Of these sites, eight were identified in *LWS*, three in *SWS1*, one in *SWS2*, and three in *RH1*; only site 234 in LWS is a known spectral tuning site, although four others are within three amino acids from a known spectral tuning site (Table 1; Data S1; Table S3). Nine of the 15 sites were identified to be under selection in both D and DC foreground groups, five were only identified to be under selection in the D foreground, and only one site was unique to the DC foreground. Most sites were found to be under selection in only one or two branches, but several (sites 87, 169, 277 in *RH1*, and site 66 in *LWS*), were found to be under selection in three or more branches, suggesting that these sites may be of functional importance in diurnal frogs (Figs. 1 and S1).

Gene	Known spectral tuning sites in vertebrates	Codon number		Nearby spectral tuning site (bovine RH1 numbering)	Location	Foreground group under positive selection: Selection test	p-value	Number of branches (MEME only)
		this study	bovine RH1					
LWS	100, 164,181, 214, 217, 261, 269, 292, 293	66	49[a]	--	TMDI	D: MEME	<0.01	6
		76	59	--		D: MEME	0.04	1
		105	88	--		D: FEL (+)	0.04	--
		128	111	--		DC: MEME DC: FEL (+)	0.04 0.02	0 --
		183	166[a]	164	TMDIV	D: MEME D: FEL (+) DC: MEME DC: FEL (+)	0.01 <0.01 0.01 0.01	1 -- 1 --
		193	176	--	TMDIV	D: MEME D: FEL (–) DC: MEME DC: FEL (–)	0.01 <0.01 0.01 <0.01	2 -- 2 --
		234	217[a]	217	TMDV	D: MEME	0.02	0
		279	262	261	TMDVI	D: MEME DC: MEME	<0.01 <0.01	2 2
SWS1	46, 49, 52, 81, 86, 90, 91, 93, 97, 108, 109, 113, 114, 116, 118, 207	45	50	49, 52	TMDI	D: MEME D: FEL (+)	0.03 0.02	2 --
		94	99	97	ECDI	D: MEME D: FEL (–) DC: FEL (–)	0.04 <0.01 <0.01	1 -- --
		216	221	--	TMDV	D: MEME D: FEL (+) DC: MEME	<0.01 0.02 0.02	2 -- 1
SWS2 (Only sites up to 129 were analyzed)	44, 46, 49, 52, 91, 93, 94, 97, 99, 109, 116, 117, 118, 122, 164, 207, 261, 265, 269, 275, 292, 295	115	106	--	ECDI	D: MEME DC: MEME	0.03 0.03	1 1
RH1	83, 90, 96, 102, 118, 122, 124, 125, 164, 183, 189, 194, 195, 207, 208, 211, 253, 261, 265,	87	87	--	TMDII	D: MEME D: FEL (+) DC: MEME DC: FEL (+)	<0.01 <0.01 <0.01 <0.01	3 -- 2 --
		169	169[a]	--	TMDIV	D: MEME D: FEL (+)	<0.01 <0.01	4 --

	269, 289, 292, 295, 299, 300, 308					DC: MEME DC: FEL (+)	<0.01 <0.01	8 --
		277	277[a]	--	TMDVI	D: MEME DC: MEME	<0.01 <0.01	2 3

[a]Amino acid sites reported by Schott et al. 2022.

Table 1. Amino acid sites in four opsin genes that were detected to be under positive selection by HyPhy analyses when specifying the Diurnal (D) or the Diurnal and Colorful foreground (DC). We aligned sequences against bovine rhodopsin (NP_001014890.1) to make comparisons with known spectral tuning sites (see Table S3 for tuning site references). More details regarding the phylogenetic patterns of amino acids at these sites can be reviewed in Fig. 1 and Fig. S1. Several sites were found to be under episodic positive selection (by MEME) and under negative selection (by FEL); thus, we report all significant FEL results that correspond to sites identified by MEME, and note each as indicative of positive (+) or negative (–) selection. ECD, extracellular domain; TMD, transmembrane domain; --, not available. Reported p-values for MEME have been corrected for multiple testing using Holm-Bonferroni; "<0.01" is denoted if the p-value is smaller than 0.01; full test results are available in Data S1.

Site 277, one of the three sites detected in *RH1*, was reported to be under episodic positive selection in both diurnal (D, two branches) and diurnal and brightly colored (DC, three branches) foregrounds. However, upon reviewing the alignment, we noted that there were no non-synonymous changes on the branches identified by MEME (*Atelopus spurrelli* and Node 33, the ancestral branch leading to *Atelopus spurrelli, A. glyphus, A. limosus,* and *A. varius*; Fig. 1). Instead, these branches have two mutations that do not result in an amino acid substitution (Ser-AGC → Ser-TCC), but likely require a nonsynonymous intermediate that is not recovered in our analysis.

To visually compare Hyphy results between diurnal (D) and colorful diurnal (DC) foreground groups, we categorized each amino acid site (in each gene) by its MEME and FEL results (Fig. S2). As expected for genes with functional constraints, many amino acid sites were found to be under negative selection by FEL (Fig. S2). A large proportion of amino acids were not found to be under either negative or positive selection, especially when specifying the DC foreground (e.g., compare our results to those of Gendreau *et al.* [2021]). We conservatively interpret the larger number of sites not under selection in the DC foreground as a reflection of its smaller sample size (N = 46 vs. 70, 13 vs. 16, 47 vs. 73, 46 vs. 71 for *SWS1*, *SWS2*, *LWS*, and *RH1*, respectively), which could have decreased our statistical power. In addition, we note that two sites (Table 1, noted with "FEL (–)") were found to be under positive selection in a subset of branches by MEME but negative selection across the phylogeny by FEL; these sites are each characterized by high conservation across the phylogeny (Figs. 1 and S1) and an amino acid change present in only one or two branches within foreground groups. Two sites in *LWS* (Table 1) were found to

be under episodic positive selection in no branches, suggesting that the signal for selection is diffuse. A diffuse signal of selection occurs when at a given site there is enough signal to report positive selection, but no individual branch rises to the level of significance.

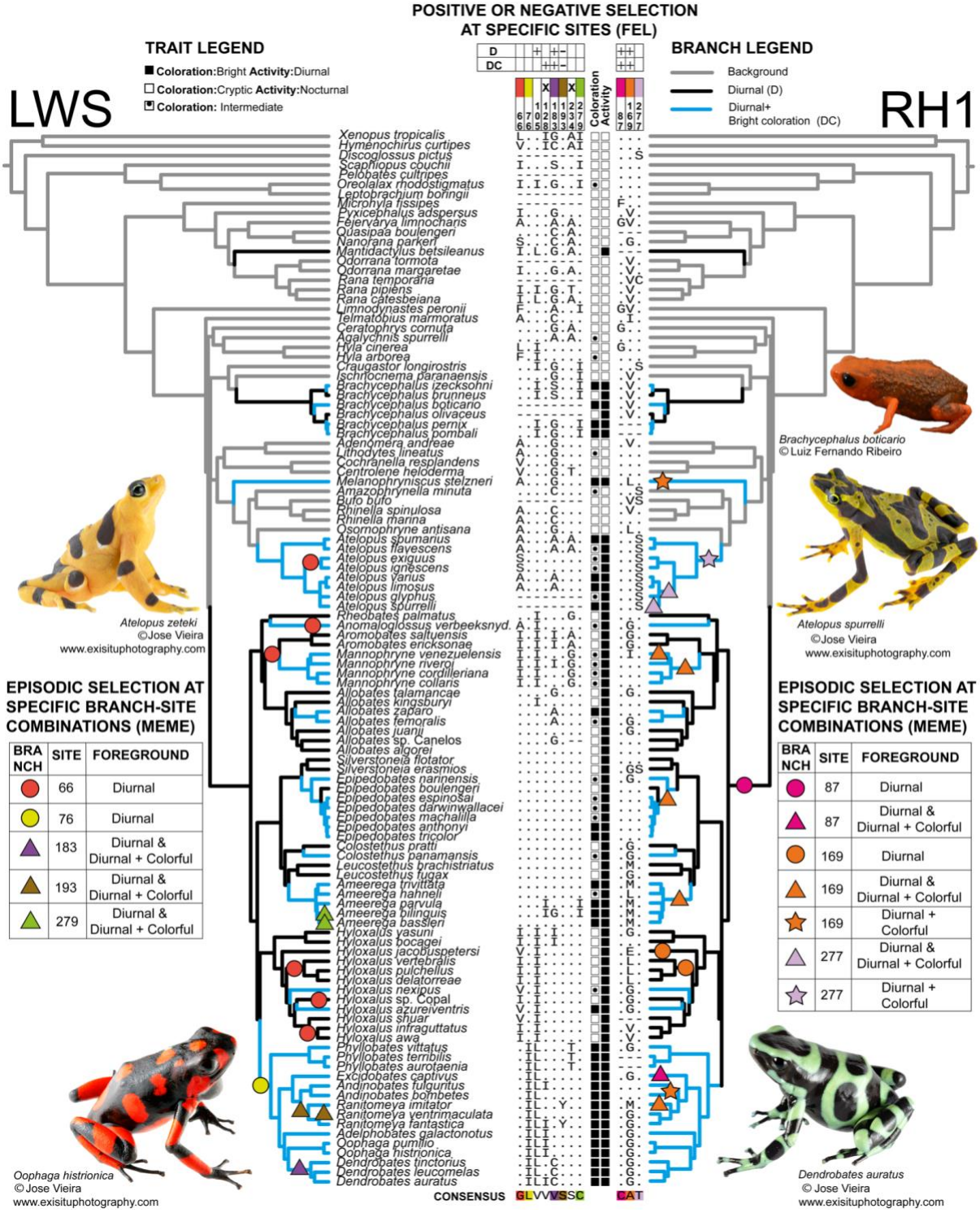

Figure 1. A summary of color and activity trait data used in analyses (see Table S1 for references) and results from HyPhy selection analyses of two opsin genes, *LWS* and *RH1* (see Fig. S1 for *SWS1* and *SWS2* and Table 1 for details). All HyPhy analyses were conducted twice using two foreground clades: D, Diurnal taxa (all non-grey branches) and DC, the subset of Diurnal taxa that are Colorful (blue branches); branches in gray correspond to the background taxa not included in analyses. Branch-site combinations that were detected by MEME (Mixed Effect Models of Evolution) as evolving under positive selection on several branches ("episodic selection") are mapped onto the phylogenetic tree using symbols; colors correspond to specific sites in the alignment. Two sites in *LWS* were significant in MEME analyses but no specific branch-site combination was reported; these are marked by "X" above the alignment. Five of the sites identified by MEME for *LWS* and *RH1* were also reported by FEL as under pervasive positive selection across the entire foreground; FEL results are included above the amino acid numbers using + to indicate positive selection and – to indicate negative selection. Site 105 was detected by FEL, but not by MEME, thus no color is provided above the alignment (see Discussion). The abbreviated species name corresponds to *Anomaloglossus verbeeksnyderorum*.

Verifying absence of SWS2 *in poison frogs.* Using synteny analyses and BLAST, we found that *SWS2* is located in a syntenic block with *LWS* and mecp2 in the ancestor of all tetrapods, in the ancestor of all amniotes (Fig. 2A), and in five frog families for which genomic data currently exist (Fig. 2B: Bufonidae, Leptodactylidae, Eleutherodactylidae, Pipidae, and Ranidae). The *O. pumilio* genomic scaffold containing *LWS* was also syntenic with other amphibians (two short and highly conserved regions between *SWS2* and *LWS* could be aligned between *Nanorana* and *O. pumilio* [Data S2]), but we could not identify any coding region of *SWS2*. The more complete scaffold of this region from *R. imitator* included the gene *mecp2* which is expected to be upstream of *SWS2*, yet we were also unable to find *SWS2* on this scaffold (Fig. 2B). In fact, we could not detect an *SWS2* gene or pseudogene on any scaffold in *O. pumilio* or *R. imitator* genomes (Table S4). In contrast, using the same methods we were able to detect *SWS2* upstream of *LWS* in *Rhinella* (Fig. 2B).

Further, we were unable to reconstruct *SWS2* from any dendrobatid species using our bait-capture data. This might suggest that our *SWS2* sequence baits (designed using a consensus sequence matrix) were not similar enough to capture this gene in dendrobatids, but we had no issues obtaining sequences from all other clades including the other aposematic species of *Atelopus* and *Brachycephalus* (Fig. S1). Finally, we were unable to amplify *SWS2* from *O. pumilio* eye cDNA. Thus, the most parsimonious explanation is that a functional *SWS2* gene is not present in *O. pumilio* or *R. imitator* and that the *SWS2* gene may have been pseudogenized (to a point beyond recognition) or lost in the ancestor of dendrobatids between 70 and 40 Mya.

Figure 2. A) *SWS2* is found in a syntenic block with *LWS* in the ancestors of all tetrapods (block 355) and in the ancestor of all amniotes (block 65). B) The region in *Xenopus tropicalis* (chromosome 8, NC_030684:32108538-32360324) shows synteny with *Rana (R.) temporaria* (chromosome 9, NC_053497.1:22641469-22170306; Ranidae), *Nanorana parkeri* (unplaced scaffold, NW_017306743:511492-806940; Ranidae), *Rhinella marina* (contig ctg22529_RHIMB, ONZH01019223.1:1-80000; Bufonidae), *Bufo bufo* (chromosome 8, NC_053396.1:25948637-26357822; Bufonidae), *Eleutherodactylus coqui* (chromosome 9,

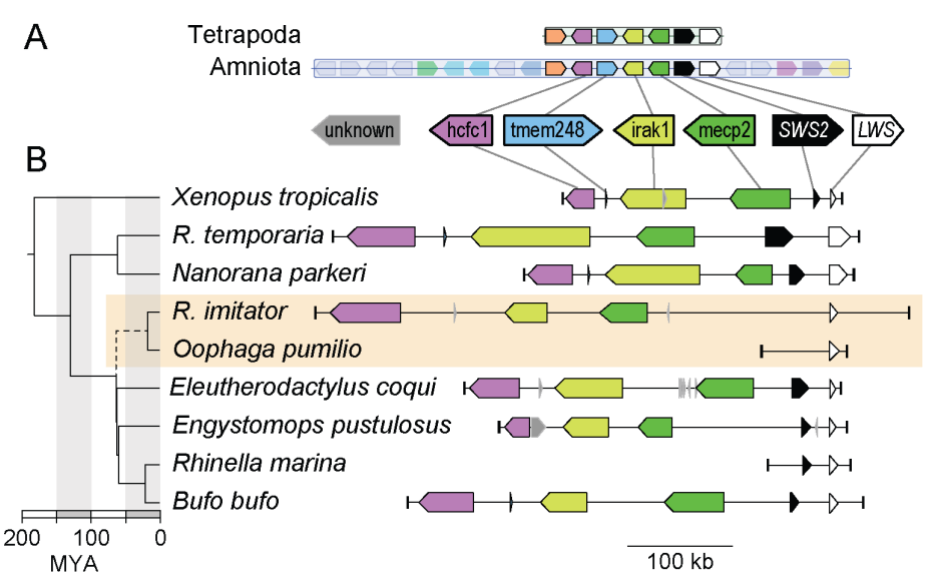

CM034094.1:11013102-11351932; Eleutherodactylidae), *Engystomops pustulosus* (chromosome 10, CM033650.1:68367373-68196643; Leptodactylidae), which also all contain *SWS2, mecp2, irak1, tmem187,* and *hcfc1* upstream of *LWS*. However, *SWS2* is absent in the scaffold containing *LWS* in two dendrobatid genomes (*Oophaga pumilio* [scaffold70671:1-49101] and *Ranitomeya* [*R.*] *imitator* [CAJOBX010072427.1, scaffold934:531,527-1]). A dated chronogram (Feng et al. 2017) indicates that *SWS2* may have been lost in the ancestral lineage (dashed line) leading to Dendrobatidae (orange box), between ~70 and 40 million years ago (Mya). Where coding regions were identified in genome assemblies, but not annotated, we added annotations manually using blastp and blastn. Coding regions in grey had ambiguous blast results and thus were left without annotations.

Discussion

Animals that rely on color-based signals (i.e., detecting ripe fruits; Melin et al. 2009) or perceiving sexual signals (Carleton et al. 2005) are expected to have a suite of opsins that are tuned to maximally perceive the relevant signal under the specific light environments that are present in the habitats where they live. Anurans constitute a powerful model for studying the evolution of opsins because they occupy diverse ecological niches. Anurans can be fossorial, terrestrial, aquatic, or a combination of these depending on life stage; they can be nocturnal, diurnal, or crepuscular; and they exemplify extreme cases of both crypsis

and aposematism (Stebbins and Cohen 1997; Wells 2007). Consequently, anuran taxa likely possess a wide range of visual system sensitivities and acuities that facilitate comparative approaches to identify adaptations to different ecological contexts (Donner and Yovanovich 2020; Schott et al. 2022). While color-based signaling occurs in several species of poison frogs (Dendrobatidae) and might exist in some harlequin toads (*Atelopus*) and pumpkin toadlets (*Brachycephalus*), very little is known in general about how anuran visual capabilities are related to intraspecific communication and signaling. Here, we present a taxonomically and ecologically comprehensive dataset of the four visual opsin genes (*LWS, SWS1, SWS2,* and *RH1*) for 116 anuran species spanning 20 families. Our analyses report 15 amino acid sites as under positive selection in diurnal species. We find no compelling evidence that conspicuous coloration is linked to the spectral tuning of visual pigments in our focal taxa. Moreover, our results provide evidence for the loss of the *SWS2* gene in the ancestor of Dendrobatidae between 70–40 Mya, an event that coincides with the evolution of diurnal activity patterns in the clade.

Selection analyses. Most of the amino acid sites inferred to be under positive selection in the four opsin genes occur in transmembrane domains (Table 1). Transmembrane domains impact the tertiary structure, thermal stability, and properties of the retinal-binding pocket (Andrés et al. 2001; Yokoyama et al. 2006). Therefore, spectral sensitivity is related directly to interactions between the amino acid residues in the transmembrane domains and the chromophore (Yokoyama et al. 2006). Although it is possible that replacements at these sites might influence spectral tuning in frogs, without more experimental data, their implications are difficult to interpret. For this reason, we conservatively discuss their possible role in anuran vision below.

Of the sites we found to be under positive selection, only one in *LWS* is a known spectral tuning site (amino acid 234 in our study, 217 in bovine *RH1*, and 233 in the human *LWS*), which has been previously shown to play a role in the differentiation of the spectral sensitivities between the red (*LWS*) and green pigments (*MWS*) in humans and other mammals (Yokoyama and Yokoyama 1990; Asenjo et al. 1994; Fasick and Robinson 1998; Yokoyama and Radlwimmer 2001). It was also reported to be under selection in a recent study on anuran visual opsin gene evolution (Schott et al. 2022), confirming that this site also likely plays a role in *LWS* spectral tuning in anurans. In our study, MEME detected episodic positive selection on this site without indicating any specific branches under selection, suggesting a diffuse signal of selection across the tree (Fig. 1; Table 1). Amino acid substitutions at this site could be responsible for shifting the sensitivity of *LWS* in frogs. A serine-to-alanine substitution at this site is reported to potentially contribute to the spectral difference between the middle- and long-wave-sensitive visual pigments in new world primates and humans (Neitz et al. 1991; Asenjo et al. 1994; but see Hiramatsu et al. 2004). In our alignment, several amino acid substitutions are present at this site in the dendrobatid genera *Mannophryne, Rheobates, Aromobates,* and *Phyllobates*, as well as two species of

Atelopus and several outgroups. Experimental validation will be necessary to interpret their potential effects on visual acuity.

Considering the general lack of data on spectral tuning sites in frog opsins, it is possible that other sites we identified to be under positive selection (Table 1) are directly or indirectly involved in spectral tuning in anurans but have not yet been characterized. For example, site 99 in *SWS1* is close to spectral tuning site 97 (Yokoyama 2008), previously reported as underlying changes in the λ_{max} of the violet-sensitive opsin in some fish (Phillips et al. 2015; Miyazaki et al. 2017). Sites 166 and 262 in *LWS* are close to known spectral tuning sites 164 and 261 (Escobar-Camacho et al. 2020); mutations at each or all of these sites can shift λ_{max} of *LWS*. For example, in humans, the substitution of serine by alanine at site 164 reduced λ_{max} of *LWS* by 7 nm (Asenjo et al. 1994). Moreover, S164A in conjunction with H181Y, Y261F, T269A and A292S (following bovine rhodopsin numbering) shifts the λ_{max} of *LWS* downward by up to 50 nm (Yokoyama and Yokoyama 1990; Yokoyama and Radlwimmer 1998). The S164A substitution is present in the sequence of *O. pumilio*, and although it was not found to be under selection, it may account for the blue-shift of λ_{max} in *LWS* reported in this species relative to other frogs (Siddiqi et al. 2004). Similarly, site 50 in *SWS1* is adjacent to a spectral tuning site at position 49. Although amino acid replacements at site 49 do not shift the maximum wavelength by themselves, when they occur in conjunction with other substitutions, a shift in sensitivity occurs in the mouse *SWS1* (Yokoyama and Tada 2003). Therefore, sites listed in Table 1 may work alone or together to shift the wavelength sensitivity of anuran opsins. Finally, we highlight that sites 87, 169, and 277 in *RH1* were each identified to be under positive selection in three or more branches (Table 1, Fig. 1). Although none of these sites are known to be involved in spectral tuning in other vertebrates (Table 1), we speculate that they may be of functional importance in frogs. Site 169 appears to be especially promising, as it was found to be under selection in 8 of the Diurnal and Colorful lineages. Experiments using site-directed mutagenesis would help verify which sites are important for spectral tuning in anurans and other amphibians.

Of the 16 sites identified by Schott and colleagues (2022) to be under positive selection in opsin genes of anurans, we identified 5 of these same sites as under selection in our focal diurnal frog clades (Table 1). It is plausible that we did not find the other 11 sites to be under positive selection because of the differences in the number of taxa (i.e., 116 in our study vs. 33 in theirs) or the specific focus on diurnal species in our study. Schott et al. (2022) also discussed additional variation in other known spectral tuning sites, but we didn't find any of these sites to be under selection in our foreground groups.

In diurnal frogs, the majority of sites in each opsin gene were identified to be under negative selection (Fig. S2), most likely due to functional constraints on opsins and rhodopsins (Goldsmith 1990; Borges et al. 2015). In contrast, most sites in the colorful subset of diurnal frogs ("DC") were not identified to be under either positive or negative selection (Fig. S2). We hypothesize that this pattern arose because of the smaller sample size of colorful frogs resulting in less power in each analysis.

Only one of the fifteen sites identified to be under positive selection was unique to the diurnal and colorful frog foreground lineages (Table 1), demonstrating a lack of support for the hypothesis that origins of colorful signals in focal frogs have introduced selection for changes in their visual abilities through sexual selection. Instead, our results suggest that diurnality appears to be more strongly associated with opsin evolution in aposematic frogs and their ancestors (Figs. 1 and S1). Nevertheless, we note that our analyses of selection may be limited by sample size, especially for the group of diurnal and colorful anurans. The recent discovery of an *LWS* duplication on the sex chromosome of the African bullfrog (*Pyxicephalus adspersus*) supports the possibility of sex-specific visual adaptation in frogs (Schott et al. 2022). A study reviewing variation in opsin sensitivity within species to identify sex-specific variants (e.g., like McCulloch et al. 2016)) that may be related to sexual selection could help verify this hypothesis.

Loss of SWS2 *in Dendrobatidae and the implications for their visual ecology.* Based on our inability to sequence *SWS2* from an *O. pumilio* eye transcriptome, the complete absence of *SWS2* from bait-capture data from all major lineages of Dendrobatidae (60 species), and our failure to identify any trace of an *SWS2* gene or pseudogene in the *O. pumilio* and *R. imitator* genomes, we hypothesize that dendrobatids lost this gene early in their history. Such gene-loss events are not surprising as other comparative genomic studies have shown (Borges et al. 2015; Xu et al. 2021). Yet the most important question is how such a loss influenced phenotypic evolution after the event. To answer such a general question, we can explore some specific ones. First, how has *SWS2* loss contributed to the differentiation of dendrobatids from other frog lineages? Our data suggest that only dendrobatids lost *SWS2*, so we propose that the loss of *SWS2* is a synapomorphy of Dendrobatidae (i.e., Aromobatidae + Dendrobatidae sensu Grant et al. [2006]). The limited empirical data from anurans suggest that *SWS2* expression is restricted to green rods (Yovanovich et al. 2017; Mohun and Davies 2019). However, green rods are absent from the *O. pumilio* retina (Siddiqi et al. 2004). Thus, the loss of *SWS2* suggests that under low light levels, dendrobatids might be less capable of discriminating color (scotopic vision) than other diurnal frogs. To our knowledge, color vision and its molecular underpinnings in the other two focal clades of this study, *Atelopus* and *Brachycephalus*, remain unstudied.

Second, how did *SWS2* disappear from the genome of ancestral dendrobatids? Based on our results, we could not find a *SWS2* pseudogene (i.e., nonfunctional segments of DNA that resemble functional *SWS2*) in the available genomic data, while close relatives of dendrobatids do have a functional *SWS2* (Fig. 2). Hyloidea is a superfamily of frogs that contains dendrobatids; the last ancestor of hyloids existed about ~70 Mya (Feng et al. 2017). The approximate age of the crown clade of Dendrobatidae is ~40 Mya (Feng et al. 2017) and thus *SWS2* must have been lost between 40–70 Mya. Two alternative explanations exist for the loss of *SWS2* during this 30-My timeframe: (1) The ancestor of dendrobatids

had a functional gene which pseudogenized and changed beyond recognition during that period, or (2) *SWS2* was lost without pseudogenization. Given the lack of evidence of *SWS2* pseudogene relics, the most parsimonious explanation is a complete deletion of the gene.

Third, was the loss of *SWS2* consequential in that it affected other aspects of dendrobatid vision? Other diurnal hyloid clades in our dataset have not lost *SWS2*: all *Atelopus* and *Brachycephalus* frogs maintain this gene. Whether these clades have the green rod cell type (which expresses *SWS2*) remains unknown. Nevertheless, dendrobatids are known to differ in at least two visual properties from close relatives. First, the lenses of some dendrobatid species (*Oophaga pumilio, Epipedobates tricolor, Dendrobates auratus, D. leucomelas, Allobates femoralis* and *Adelphobates castaneoticus*) transmit less short-wavelength light (lens $\boldsymbol{\lambda}_{t50}$ 413–425 nm; except for *D. leucomelas* lens $\boldsymbol{\lambda}_{t50}$ 326 nm) than those of bufonids (*Rhinella marina, R. icterica, R. ornata, Bufo bufo, Rhaebo guttatus, Sclerophis maculata*, and *Atelopus varius* lens $\boldsymbol{\lambda}_{t50}$ 331–365 nm) and brachycephalids (*Brachycephalus rotenbergae, Ischnocnema parva, I. henseli* lens $\boldsymbol{\lambda}$t50 314–356 nm) (Donner and Yovanovich 2020; Yovanovich et al. 2020; Thomas et al. 2022). Because the typical peak wavelength sensitivity of *SWS2* rods (~430 nm; Yovanovich et al. 2017) is much closer to the limit of lens transmission in dendrobatids than other frogs, it is plausible that lens transmission properties were adjusted in some species following the loss of *SWS2.* Additionally, in *O. pumilio*, the short-wavelength-sensitive cone (likely *SWS1*), which absorbs light wavelengths around 430 nm in other anurans (Yovanovich et al. 2017), was found to absorb light at 466 nm (Siddiqi et al. 2004), suggesting that it has undergone a shift in spectral sensitivity. Further investigation of these patterns will clarify whether loss of *SWS2* in dendrobatids in combination with a diurnal lifestyle led to altered lens transmission properties and a change in *SWS1* wavelength sensitivity, or vice versa.

Despite the apparent loss of *SWS2* in dendrobatid frogs and the lack of *RH2* pigment in amphibians (Mohun and Davies 2019), microspectrophotometry data revealed an *MWS* photoreceptor in the *O. pumilio* retina (Siddiqi et al. 2004). We speculate that these frogs are instead using *RH1* in those photoreceptors as the microspectrophotometry absorbance graphs for rods and MWS cones appear nearly identical (Siddiqi et al. 2004). Whether this is the case and if there are any modifications to the *RH1* pigment or to any proteins in the *O. pumilio MWS* cone phototransduction pathway required to make the rod protein function in cone cells requires further investigation. Empirical data of spectral sensitivity in frogs is sparse and further studies using microspectrophotometry of isolated poison frog rods and cones will be necessary to recapitulate the evolution of vision in frogs (Donner and Yovanovich 2020).

Conclusion. Our results fill gaps in our knowledge by illustrating how shifts in ecology and life history may have affected vision in amphibians. While we found evidence for diurnality as a potential driver of opsin evolution in anurans, the absence of unique signatures of selection on opsin genes of colorful anurans suggests that the origins of warning signals in aposematic Dendrobatidae, *Atelopus,* and

Brachycephalus have not strongly selected for changes in frog vision, at least not in ways that we could detect in the present study. Further work is needed to elucidate the functional consequences of the loss of *SWS2* in Dendrobatidae. Like Donner and Yovanovich (2020), we expect that additional studies of opsin evolution in amphibians will reveal non-canonical visual adaptations and broaden our understanding of the many ways in which animals adapt to diverse light environments.

Materials and Methods

Bait capture design, library preparation, and sequencing. Using publicly available sequences (see Table S1), previously generated transcriptomes (Santos et al. 2018), and sequences from a frog transcriptome project described in Santos et al. (2018), we designed a custom bait-capture array with myBaits® (Arbor Biosciences). The 120-bp baits were synthesized at >10x tiling across all exons of the genes of interest.

Tissues from representative species of Dendrobatidae, *Atelopus*, and *Brachycephalus* and their relatives were obtained from the field or from museum collections (see Table S1 for source information), under approved protocols (UT Austin AUP-2012-00032 and AUP-0709210, STRI 200715122207, 2015-00205 Tulane #0453) and collection permits (001-13 IC-FAU-DNB/MA and 001-11 IC-FAU-DNB/MA [Ecuador], IBD0359 Res 1177-2014 and Isla Gorgona PIDB DTPA 020 - 16 Res 061-16 [Colombia], and SE/A-47-07 and CITES export permit SE/A-47-07 [Panama]). Tissue samples from Ecuador and Peru were loaned by Luis A. Coloma (Fundación Otonga and Centro Jambatu de Investigación y Conservación de Anfibios; Ecuador) and César Aguilar (Universidad Nacional Mayor de San Marcos; Lima, Peru).

DNA was extracted using Qiagen DNeasy kits (Germantown, MD). DNA quality was reviewed with a 0.8% electrophoresis gel and highly degraded samples were excluded. RNA was removed from extractions with RNAse A (E1008, Zymo Research, Irvine, CA), and extractions were further purified and concentrated with Genomic DNA Clean and Concentrate (D4011, Zymo Research) and then quantified using a Qubit 3.0 fluorometer (Thermo Fisher Scientific, Waltham, MA) following manufacturer protocols. Given the large size of amphibian genomes, we used between 400 and 1600 ng of starting DNA for each sample for library preparation. DNA was sheared to an average size of 300bp using a Covaris S2 Focused-ultrasonicator (Covaris, Inc, Woburn, MA; settings as Intensity: 5; Duty Cycle: 10%; Cycles per Burst: 200; Time: 50s; Temp: 7C; Water Level: 12; Sample Volume: 50 µL). Whole-genome libraries were prepared from sheared samples using the KAPA Hyper Plus library preparation kit (KK8514, Roche Diagnostics, Santa Clara, California), NEBNext Multiplex Oligos for Illumina (E7600, New England BioLabs, Ipswich, MA), home-made SPRI beads (Rohland and Reich 2012) (pers. comm. Lydia Smith), and manufacturer protocols. Uniquely barcoded libraries from 4–10 closely related species were pooled to a total of 1.6–5µg DNA and then size-selected for an insert size of 250 ± 25 bp (total length with 120-bp adaptors: 345 ± 25 bp) using a Blue Pippin (Sage Science, Beverly, MA) and 2% gel cassette. For samples with low concentrations, a second batch of libraries were constructed with the same

protocol, except that these were size-selected to 250 ± 50 bp with a 1.5% gel cassette (total length with 120-bp adaptors: 370 ± 50 bp). All size-selected libraries were cleaned with Qiagen MinElute PCR purification kits, eluted in 10 µL, and quantified with Qubit 3.0.

7µL of each pooled library set (50–275ng/pool) was then hybridized with our custom myBaits biotinylated RNA, C_0t-1 DNA, and xGen® Universal Blockers–TS Mix (1075474, Integrated DNA Technologies, Redwood City, CA) according to myBaits v4.01 recommended protocols. Because amphibian genomes are large and contain many repetitive sequences, we used a large amount of starting DNA (1.6–5µg at size selection) and a larger quantity of blocking oligos than described in the manufacturer's protocol (8ug human C_0t-1 and 8µg salmon C_0t-1 per hybridization reaction). We also used the xGen blockers rather than those provided in the myBaits kit. Following hybridization with C_0t-1, universal blockers, and baits for 36 h, pooled libraries were washed and cleaned with DynaBeads MyOne Streptavidin C1 beads (65002, Thermo Fisher Scientific). 12–17µL of resulting libraries (including beads) were amplified using the NEBNext Illumina primers (that came with the multiplex oligos) and the KAPA Library Amplification Kit (KK2611, Roche Diagnostics) in two separate PCR reactions with 15-17 cycles. These were purified and eluted in 10µL with the Qiagen MinElute purification kit. Duplicate PCR reactions and libraries from all 97 samples were normalized by concentration and according to the number of samples per pool and then sequenced across two lanes of the Illumina HiSeq4000 at the Genome Sequencing and Analysis Facility (GSAF) at University of Texas at Austin, yielding approximately 4M reads per sample.

Assembly of opsin genes. The quality of reads was checked with FastQC (Andrews 2010), barcodes were excluded with Trimmomatic (Bolger et al. 2014) and, because combining multiple assembly methods better characterize multi-gene families (Holding et al. 2018), the reads were assembled with default parameters for *de novo* with MEGAHIT (Li et al. 2015), Trinity (Grabherr et al. 2011) and SPAdes (Bankevich et al. 2012). Final assemblies were reduced using CD-HIT set to >98% similarity. Reduced assemblies were annotated using a custom sequence library generated with the opsin sequences used to design the baits and the software suite provided by BLASTX. Reference sequences for BLASTX were derived from amphibian opsin genes available in GenBank: *Xenopus laevis* (Pipidae), *Nanorana parkeri* (Dicroglossidae) and other species with opsin sequences (e.g., *Rana catesbeianus* [Ranidae]). Any sequence matching one of the reference opsin genes with an e-value $<10^{-6}$ was pulled out for downstream analyses.

Given that we *de novo* assembled genomic DNA that was captured using baits designed from mRNA, the sequences were often only partially assembled, and some shorter sequences were identified erroneously by BLASTX. We used the program BLAT v.36x2 (Kent 2002) with reference sequences from the *Nanorana parkeri* genome (*LWS*, XM_018560714.1; *SWS1*, NW_017306744.1; *SWS2*,

NW_017307939.1; *RH1*, NW_017306456.1) to verify sequences from our dataset that were putatively identified as opsins using BLASTX as described above. A BLAT server was prepared using *N. parkeri* reference sequences with the "-trans" option to translate the database into protein for all six reading frames. Then BLAT was run with options "-t=dnax" and "-q=dnax" to specify that the format of the database and query were both DNA sequences translated in six frames to protein. Sequences that matched *N. parkeri* references were pulled out from the BLAT results file generated using "-o=pslx". These query sequences were then aligned to the reference genome using MAFFT v47.19 (Katoh and Standley 2013) with the options "--auto" and "--adjustdirection". The smaller fragments whose sequences did not align to the exons were manually removed, and exons from the same individual of each species were merged.

For most of these genes, some edges of exons and several short exons were still missing from the assemblies. To recover the sequences or fill these gaps, we implemented an *in silico* target capture using MITObim (Hahn et al. 2013). For this procedure, we used the recovered exon sequences as bait sequences and the raw exome capture as target data. We included the following parameters "--quick" (starts process with initial baiting using provided fasta reference), "--mismatch" (% number of allowed mismatches in mapping), and "--kbait" (set kmer for baiting stringency). For the last two parameters we used low stringency (12-17 and 10-15, respectively) to bait more raw reads beyond those obtained from standard assemblers. This approach allowed MITObim to progressively expand the extremes of the bait sequences beyond the original gene reconstructions. The resulting sequences were then aligned with the original sequence matrices for each gene and full sequences from NCBI references (e.g., *Xenopus*, *Nanorana*, and *Rana*). In most cases, these extended sequences overlapped and were merged with the original ones to recover the missing regions. Lastly, we generated a clean alignment containing only coding regions that we used for the subsequent analyses. Raw sequencing coverage for *SWS2* past position 389 was low (perhaps because probes designed for that region did not effectively pull-down exons compared to other probes), so we exclude the remaining sequence to avoid any potential errors in its reconstruction.

Gene tree construction. To check for any sequence contaminants, misidentifications, or assembly errors, we estimated a gene tree for each opsin, partitioned by codon position (length of alignment divided by three, because three bases constitute to a codon), using raxml-ng v.0.9.0 (Kozlov et al. 2019), the GTR+G model, and 200 bootstrap replicates to assess support. We found several sequences of different species to be identical for each gene, although in each case the identical sequences were from closely related species. For *LWS*, there were two sets of identical sequences: *Atelopus glyphus* and *A. spurrelli; Brachycephalus boticario* and *B. olivaceus*. For *SWS1* and *SWS2*, there was one set of identical sequences for each gene: *Atelopus glyphus, A. limosus* and *A. varius* for *SWS1*; *Brachycephalus pernix* and *B. pombali* for *SWS2*. For *RH1*, we found two sets of identical species: *Brachycephalus pernix* and *B. pombali; Phyllobates aurotaenia* and *P. terribilis*. Because there are no genomes for these species, it was

not possible to verify the sequences, so we conservatively excluded all identical sequence sets from the following analyses.

Determination of aposematic and diel habits. Data on frog coloration and time of activity was compiled from primary and secondary literature, including species descriptions, taxonomic revisions, and books (see Table S1 for references). See Supplementary Information for details on the activity and coloration states for each species used in our analysis and the associated sources.

Activity patterns were categorized as diurnal or nocturnal, with the latter category conservatively including species with exclusively crepuscular or mixed activity patterns. When not clearly stated, the time of activity was inferred from reports on time of calling, breeding activity, and behavior (asleep or active) at the time of collection. Diurnal groups include our focal clades Dendrobatidae, *Atelopus, and Brachycephalus,* as well as *Mantella baroni*, *Mantidactylus betsileanus*, and *Melanophryniscus stelzneri*. The following genera were classified as nocturnal: *Adenomera, Agalychnis, Amazophrynella, Amietia, Bufotes, Centrolene, Ceratophrys, Cochranella, Craugastor, Discoglossus, Fejervarya, Hyla, Hymenochirus, Ischnocnema, Leptobrachium, Limnodynastes, Lithodytes, Microhyla, Nanorana, Odorrana, Oreolalax, Osornophryne, Pelobates, Pyxicephalus, Quasipaa, Rana, Rhinella, Scaphiopus, Telmatobius,* and *Xenopus*.

Coloration was categorized as bright, intermediate, or cryptic based on the proportion of the dorsal, ventral, and hidden surfaces of the body such as flanks, groins, shanks, armpits, and soles of hands and feet presenting bright colors (i.e., red, orange, yellow, blue) or bearing colorful, contrasting markings, according to human perception. Green was considered bright or intermediate only when on a contrasting background (e.g., *Centrolene heloderma* is cryptic, while *Atelopus spumarius* is intermediate). When using species descriptions to determine the color category we only used the information that described coloration in life. We note that human detection and discrimination of color might not be equivalent to what ecologically relevant organisms who exert selective pression on our focal taxa might consider colorful or cryptic, such as predators, competitors, and potential mates. However, human color perception largely overlaps with visual capabilities of other vertebrates except for those that can see into the UV range or at very low ambient light conditions (Douglas 2010). Accounting for color recognition separately for each of these organisms is beyond the scope of this study. We considered brightly colored taxa to be those that present conspicuous coloration or colorful and contrasting markings covering approximately 75% or more of the dorsal, ventral, and hidden surfaces of the body (e.g., *Ameerega parvula*, *Oophaga histrionica*, *Melanophryniscus stelzneri*). The intermediate coloration category includes species with conspicuous coloration present on the ventral surface but not behaviorally displayed (e.g., no known unken reflex as in *Atelopus ignescens*; Rößler et al. 2019) and/or that bear colorful, contrasting markings that are small and cover approximately 30–75% of the dorsum and/or hidden surfaces of the body including the soles of

hands and feet. This group included several dendrobatids (e.g., *Epipedobates machalilla, Mannophryne riveroi, Amereega hahneli, Hyloxalus nexipus*), some bufonids (e.g., *Atelopus flavescens, Ate. glyphus*) and one species of hylid (*Agalychnis spurrelli*). Species that did not fit either the bright or intermediate categories were considered to have cryptic coloration.

Analyses of selection. An updated phylogeny of the focal taxa was derived from alignments provided in the two largest phylogenetic reconstructions of amphibians (Pyron 2014; Jetz and Pyron 2018). Both alignments were appended, and taxa not included in our analysis were removed, duplicate taxa were also removed by choosing the one with more sequence data, and taxonomic nomenclature was updated following (AmphibiaWeb 2022). The final sequence alignment was realigned with MAFFT (Katoh and Standley 2013), then reviewed and adjusted manually, particularly the mitochondrial ribosomal gene sequences. Multiple alignment programs usually provide a good starting point, but they usually need to be examined and adjusted by eye (Baum and Smith 2013). The optimized alignment was then used for phylogenetic estimation. A maximum likelihood tree was estimated using IQ-TREE2 2.1.3 (Minh et al. 2020) with five replicate runs. The tree was constrained so that the topology among the families of Hyloidea matched that found by Feng et al. (2017) and Hime et al. (2020). This method was preferred because the trees presented in Pyron (2014) and Jetz and Pyron (2018) are largely dictated by the abundance of data from mitochondrial genes. In contrast, the trees found by Feng et al. (2017) and Hime et al. (2020) are based on 100-1000s of nuclear genes and no mitochondrial data. The sequences were partitioned by gene and codon position and the best partitioned model was determined using -TESTMERGE option (Chernomor et al. 2016; Kalyaanamoorthy et al. 2017) within IQTREE2. Ultrafast bootstrap values (Hoang et al. 2018) were calculated using 50000 replicates and were plotted on the best likelihood tree. The data matrix, IQTREE2 scripts, constraint tree, and analysis log files are included in Supplementary Materials Data S3 in the folder IQTree.

For each HyPhy analysis, we pruned the tree using the 'ape' R-package (Paradis and Schliep 2019) to contain the subset of species available for each opsin gene. In some cases, we replaced a tip in the tree with a closely related species that was used in our study (see Table S1 for details). We then used the resulting tree as the backbone for two types of site-based selection analyses (with α set to 0.05) in HyPhy version 2.1.2 (Kosakovsky Pond et al. 2005): FEL, which estimates the rate of synonymous (*dS*) and non-synonymous (*dN*) substitutions per site with maximum likelihood and compares them using likelihood ratio tests (Kosakovsky Pond and Frost 2005); and MEME, a mixed-effects maximum likelihood approach, to test for episodic or diversifying selection using a branch model (Murrell et al. 2012).

We designated two sets of focal (foreground) clades in which to detect selection: 1) diurnal frogs, including all Dendrobatidae, all *Atelopus*, all *Brachycephalus*, and two other diurnal species included in

our study, namely *Melanophryniscus stelzneri* and *Mantella baroni*; and 2) diurnal frogs with bright or intermediate coloration, including all *Epipedobates*, all *Ameerega*, *Colostethus panamansis*, *Hyloxalus azureiventris*, *H. nexipus*, all Dendrobatinae, *Allobates zaparo*, *A. femoralis*, *Anomaloglossus verbeeksnyderorum*, *Mannophryne riveroi*, *M. venezuelensis*, *M. collaris*, *M. cordilleriana*, all *Atelopus* (with the exception of *Ate. sp*, for which phenotype data are unavailable), *Melanophryniscus stelzneri*, all *Brachycephalus* (except for *B. olivaceus* and *B. brunneus*, which are both considered cryptic), and *Mantella baroni*. Following convention, the amino acid sites are numbered based on the bovine rhodopsin sequence (NP_001014890.1); sequences from each opsin gene were aligned with bovine rhodopsin using MAFFT v7.419, and the numbering of the amino acid site was determined by referring to the numbering of bovine rhodopsin starting with the start codon as 1 (see Data S1). We report our selection results referring to the location of each amino acid according to the three dimensional structure of opsins, which encompasses seven transmembrane domains (TMD I–VII), three extracellular domains (ECD I–III), three intracellular domains (ICD I–III), and the amino- and carboxyl- termini (N and C) (Palczewski et al. 2000; Table 1, Fig. 1).

Attempts to find SWS2 *in* Oophaga pumilio *and* Ranitomeya imitator. Because we did not recover *SWS2* sequences from any dendrobatid species in our bait-capture dataset, we attempted to verify whether the *SWS2* gene had been lost in this clade using three additional approaches.

1. *de novo* transcriptome sequencing of *O. pumilio*. First, we attempted to determine which opsin genes are expressed in eye tissue of *O. pumilio*. As part of another project, one eye from each of eleven *O. pumilio* populations (Aguacate, Almirante, Bastimentos "Cemetery", Bastimentos "Green", Bastimentos "Orange", Cayo Agua, Colón, Pastores, Popa, San Cristóbal, Solarte; see Maan and Cummings (2012) for population details) was taken out of RNAlater and placed immediately in Trizol (Life Technologies, Grand Island, NY). RNA was extracted according to manufacturer instructions. Equal concentrations of total RNA from each of the 11 eye samples were pooled into a single sample from which poly-adenylated RNA was isolated using the Poly(A) purist kit (Life Technologies) according to manufacturer instructions. Lack of contaminating ribosomal RNA was confirmed using an Agilent 2100 Bioanalyzer. Strand-specific libraries for 100-bp paired-end sequencing were prepared and sequenced on the Illumina HiSeq 2000 according to manufacturer library kit instructions. A total of 83,168,029 reads were obtained. We preprocessed the reads using Trimmomatic (Bolger et al. 2014) by removing adapter sequence and sequence artifacts as well as trimming low-quality nucleotides based on the Phred score (Ewing et al. 1998) greater than 20, which corresponds to a 1% sequencing error rate.

de novo sequence assembly was then completed using Trinity (Grabherr et al. 2011) on the Odyssey cluster supported by the FAS Science Division Research Computing Group at Harvard University. We remapped reads to the raw assembly using the BWA aligner (Li and Durbin 2009) and

then used eXpress (http://bio.math.berkeley.edu/eXpress/) to generate FPKM (fragments per kilobase per million mapped) scores for each contig. Low-confidence contigs that had an FPKM value of less than one were removed from the draft assembly. After removing contigs with low confidence, we used CD-HIT-EST (Li and Godzik 2006) to remove contig redundancy. Given that redundant contigs can represent alternative splice variants, polymorphisms among the pooled individuals, or sequencing errors, we used a conservative threshold of 98% sequence similarity. The final assembly was annotated using Trinotate (Bryant et al. 2017); it was found to contain only three opsin genes: *RH1*, *LWS*, and *SWS1*. The *SWS2* gene was absent. Thus, we hypothesized that *SWS2* might have been lost in the ancestor of dendrobatids.

2. *Synteny with LWS.* If the *SWS2* gene is no longer functional in dendrobatids, we predicted that remnants of *SWS2* might be detectable in genomic data as a pseudogene either near its expected location or translocated elsewhere in the genome. We thus reviewed the genomes (Rogers et al. 2018; Rodríguez et al. 2020) of *Oophaga pumilio* and *Ranitomeya imitator* (Stuckert et al. 2021) for evidence of *SWS2* using synteny and genome mining. We searched for the syntenic block containing *LWS* using Genomicus v.100.01 (Nguyen et al. 2018) with search term *opn1lw* and *Xenopus tropicalis* as the focal species. To visualize gene order in the syntenic block we used BLAST to locate *SWS2*, *LWS*, and the gene predicted to be directly upstream of *LWS*, mecp2 (methyl-CpG binding transcription factor) in *N. parkeri*, and *X. tropicalis* genomes. We hypothesized that a degraded ancestral *SWS2* sequence might be maintained in *O. pumilio* and *R. imitator* upstream of *LWS*. We mined the published genome assembly of *O. pumilio* (Rogers et al. 2018) and a re-scaffolded version of this genome (Rodríguez et al. 2020), as well as the recently published *R. imitator* genome for *LWS* using BLAST v2.10.0 (Altschul et al. 1990). We then attempted to align the scaffolds containing *LWS* against *SWS2* sequences from other amphibians using MAFFT v7.453 (Katoh and Standley 2013). We note that the *O. pumilio* scaffold contains two sections of Ns upstream of *LWS* (2093 and 2391 nucleotides long), which may inflate our perceived length of coverage of this chromosome. Likewise, it is possible that this scaffold might be misassembled and require further refinement and deeper coverage. The re-scaffolded version (Rodríguez et al. 2020) of the *O. pumilio* scaffold containing *LWS* is identical to the original and thus did not alter our conclusions. As a positive control for this analysis, we also ran our pipeline on the draft genome of *Rhinella marina*, which is known to contain *SWS2* based on our data. This analysis is implemented in the Github folder named "synteny" (see Data S4).

3. *Mining the two dendrobatid genomes for* SWS2. Because we were unable to detect *SWS2* upstream of the *O. pumilio* and *R. imitator LWS* scaffolds, we then hypothesized that the syntenic relationship between *LWS* and *SWS2* might have been broken in *O. pumilio* and *R. imitator*. Therefore, we used tblastn v2.10.0 to screen all scaffolds from the re-scaffolded genome assembly of *O. pumilio* and the draft assembly of *R. imitator* for any potential *SWS2* orthologs. This approach uncovered several candidate sequences with low E-values (<1e-10). We screened the top candidates using tblastn against

Nanorana parkeri, a well-annotated frog genome more closely related to dendrobatids than *Xenopus*. None of the candidate sequences returned *SWS2* as the most likely ortholog; the highest scoring sequences were annotated as related proteins (e.g., pinopsin, rhodopsin; Table S4). As a positive control for this analysis, we also ran tblastn on 43 known *SWS2* sequences from other frog species against *Nanorana parkeri*. As *SWS2* is known to be present in *Nanorana*, we would expect our pipeline to correctly detect and annotate these sequences. We found that the top hit from *N. parkeri* correctly identified *SWS2* as the most likely ortholog for all 43 known *SWS2* sequences (Table S4). As another positive control, we ran an identical search for *LWS*, which identified *LWS* as the top hit for 101 other frog sequences and for one of the *Oophaga pumilio* scaffolds (Table S4). Lastly, we ran the reciprocal best-hit pipeline for *SWS2* using the *Rhinella marina* genome as the query. Since *Rhinella marina* is known to contain *SWS2*, we would expect that our pipeline should identify *SWS2* in the *R. marina* genome. We found that the pipeline identifies the same contig in *Rhinella marina* that is identified in our synteny-based analysis (ONZH01019223.1) as a likely *SWS2* ortholog, while other sequences with low E-values were annotated with other related opsin genes (Table S4). This analysis is implemented in the Github folders named "SWS2_search" and "LWS_search" (see Data S4).

References

Altschul SF, Gish W, Miller W, Myers EW, Lipman DJ. 1990. Basic Local Alignment Search Tool. *J. Mol. Biol.*:403–410.

AmphibiaWeb. 2022. <https://amphibiaweb.org> University of California, Berkeley, CA, USA. Accessed 17 May 2022.

Anderson SR, Wiens JJ. 2017. Out of the dark: 350 million years of conservatism and evolution in diel activity patterns in vertebrates. *Evolution* 71:1944–1959.

Andrés A, Kosoy A, Garriga P, Manyosa J. 2001. Mutations at position 125 in transmembrane helix III of rhodopsin affect the structure and signalling of the receptor. *Eur. J. Biochem.* 268:5696–5704.

Andrews SM. 2010. FastQC: a quality control tool for high throughput sequence data. Available from: http://www.bioinformatics.babraham.ac.uk/projects/fastqc

Asenjo AB, Rim J, Oprian DD. 1994. Molecular determinants of human red/green color discrimination. *Neuron* 12:1131–1138.

Bankevich A, Nurk S, Antipov D, Gurevich AA, Dvorkin M, Kulikov AS, Lesin VM, Nikolenko SI, Pham S, Prjibelski AD, et al. 2012. SPAdes: a new genome assembly algorithm and its applications to single-cell sequencing. *J. Comput. Biol.* 19:455–477.

Baum DA, Smith SD. 2013. Tree thinking: an introduction to phylogenetic biology. Greenwood Village, CO: Roberts

Bell RC, Zamudio KR. 2012. Sexual dichromatism in frogs: Natural selection, sexual selection and

unexpected diversity. *Proc. R. Soc. B: Biol. Sci.* 279:4687–4693.

Bolger AM, Lohse M, Usadel B. 2014. Trimmomatic: a flexible trimmer for Illumina sequence data. *Bioinformatics* 30:2114–2120.

Borges R, Khan I, Johnson WE, Gilbert MTP, Zhang G, Jarvis ED, O'Brien SJ, Antunes A. 2015. Gene loss, adaptive evolution and the co-evolution of plumage coloration genes with opsins in birds. *BMC Genomics* 16:751.

Bowmaker JK. 2008. Evolution of vertebrate visual pigments. *Vision Res.* 48:2022–2041.

Bryant DM, Johnson K, DiTommaso T, Tickle T, Couger MB, Payzin-Dogru D, Lee TJ, Leigh ND, Kuo T-H, Davis FG, et al. 2017. A tissue-mapped axolotl de novo transcriptome enables identification of limb regeneration factors. *Cell Rep.* 18:762–776.

Carleton KL, Parry JWL, Bowmaker JK, Hunt DM, Seehausen O. 2005. Colour vision and speciation in Lake Victoria cichlids of the genus *Pundamilia*. *Mol. Ecol.* 14:4341–4353.

Carvalho LS, Cowing JA, Wilkie SE, Bowmaker JK, Hunt DM. 2007. The molecular evolution of avian ultraviolet- and violet-sensitive visual pigments. *Mol. Biol. Evol.* 24:1843–1852.

Chernomor O, von Haeseler A, Minh BQ. 2016. Terrace aware data structure for phylogenomic inference from supermatrices. *Syst. Biol.* 65:997–1008.

Clough M, Summers K. 2000. Phylogenetic systematics and biogeography of the poison frogs: evidence from mitochondrial DNA sequences. *Biol. J. Linn. Soc.* 70:515–540.

Cronin TW, Johnsen S, Justin Marshall N, Warrant EJ. 2014. Visual Ecology. Princeton University Press.

Cummings ME, Crothers LR. 2013. Interacting selection diversifies warning signals in a polytypic frog: an examination with the strawberry poison frog. *Evol. Ecol.* 27:693–710.

Donner K, Yovanovich CAM. 2020. A frog's eye view: Foundational revelations and future promises. *Semin. Cell Dev. Biol.* 106:72–85.

Escobar-Camacho D, Carleton KL, Narain DW, Pierotti MER. 2020. Visual pigment evolution in Characiformes: The dynamic interplay of teleost whole-genome duplication, surviving opsins and spectral tuning. *Mol. Ecol.* 29:2234–2253.

Ewing B, Hillier LD, Wendl MC, Green P. 1998. Base-calling of automated sequencer traces using phred. I. Accuracy assessment. *Genome Res.* 8:175–185.

Fasick JI, Robinson PR. 1998. Mechanism of spectral tuning in the dolphin visual pigments. *Biochemistry* 37:433–438.

Feng Y-J, Blackburn DC, Liang D, Hillis DM, Wake DB, Cannatella DC, Zhang P. 2017. Phylogenomics reveals rapid, simultaneous diversification of three major clades of Gondwanan frogs at the Cretaceous–Paleogene boundary. *Proc. Natl. Acad. Sci. U. S. A.* 114:E5864–E5870.

Gendreau KL, Hornsby AD, Hague MTJ, McGlothlin JW. 2021. Gene conversion facilitates the adaptive evolution of self-resistance in highly toxic newts. *Mol. Biol. Evol.* 38:4077–4094.

Goldsmith TH. 1990. Optimization, constraint, and history in the evolution of eyes. *Q. Rev. Biol.* 65:281–322.

Grabherr MG, Haas BJ, Yassour M, Levin JZ, Thompson DA, Amit I, Adiconis X, Fan L, Raychowdhury R, Zeng Q, et al. 2011. Full-length transcriptome assembly from RNA-Seq data without a reference genome. *Nat. Biotechnol.* 29:644–652.

Grant T, Frost DR, Caldwell JP, Gagliardo R, Haddad CFB, Kok PJR, Means DB, Noonan BP, Schargel WE, Wheeler WC. 2006. Phylogenetic systematics of dart-poison frogs and their relatives (Amphibia: Athesphatanura: Dendrobatidae). *Bull. Am. Mus. Nat. Hist.* 299:1–262.

Hahn C, Bachmann L, Chevreux B. 2013. Reconstructing mitochondrial genomes directly from genomic next-generation sequencing reads - a baiting and iterative mapping approach. *Nucleic Acids Res.* 41:e129.

Hime PM, Lemmon AR, Lemmon ECM, Prendini E, Brown JM, Thomson RC, Kratovil JD, Noonan BP, Pyron RA, Peloso PLV, et al. 2020. Phylogenomics reveals ancient gene tree discordance in the amphibian Tree of Life. *Syst. Biol.* 70:49–56.

Hiramatsu C, Radlwimmer FB, Yokoyama S, Kawamura S. 2004. Mutagenesis and reconstitution of middle-to-long-wave-sensitive visual pigments of New World monkeys for testing the tuning effect of residues at sites 229 and 233. *Vision Res.* 44:2225–2231.

Hoang DT, Chernomor O, von Haeseler A, Minh BQ, Vinh LS. 2018. UFBoot2: Improving the Ultrafast Bootstrap approximation. *Mol. Biol. Evol.* 35:518–522.

Holding ML, Margres MJ, Mason AJ, Parkinson CL, Rokyta DR. 2018. Evaluating the performance of de novo assembly methods for venom-gland transcriptomics. *Toxins* 10:249.

Hunt DM, Carvalho LS, Cowing JA, Parry JWL, Wilkie SE, Davies WL, Bowmaker JK. 2007. Spectral tuning of shortwave-sensitive visual pigments in vertebrates. *Photochem. Photobiol.* 83:303–310.

Hunt DM, Collin SP. 2014. The Evolution of Photoreceptors and Visual Photopigments in Vertebrates. In: Hunt DM, Hankins MW, Collin SP, Marshall NJ, editors. Evolution of Visual and Non-visual Pigments. Boston (MA): Springer. p. 163–217.

Hunt DM, Dulai KS, Cowing JA, Julliot C, Mollon JD, Bowmaker JK, Li WH, Hewett-Emmett D. 1998. Molecular evolution of trichromacy in primates. In: Vision Research. Vol. 38. Pergamon. p. 3299–3306.

Jetz W, Pyron RA. 2018. The interplay of past diversification and evolutionary isolation with present imperilment across the amphibian tree of life. *Nat Ecol Evol* 2:850–858.

Kalyaanamoorthy S, Minh BQ, Wong TKF, von Haeseler A, Jermiin LS. 2017. ModelFinder: fast model selection for accurate phylogenetic estimates. *Nat. Methods* 14:587–589.

Katoh K, Standley DM. 2013. MAFFT multiple sequence alignment software version 7: improvements in performance and usability. *Mol. Biol. Evol.* 30:772–780.

Kent WJ. 2002. BLAT---The BLAST-Like Alignment Tool. *Genome Res.* 12:656–664.

Kosakovsky Pond SL, Frost SDW. 2005. Not so different after all: a comparison of methods for detecting amino acid sites under selection. *Mol. Biol. Evol.* 22:1208–1222.

Kosakovsky Pond SL, Frost SDW, Muse SV. 2005. HyPhy: Hypothesis testing using phylogenies. *Bioinformatics* 21:676–679.

Koskelainen A, Hemilä S, Donner K. 1994. Spectral sensitivities of short- and long-wavelength sensitive cone mechanisms in the frog retina. *Acta Physiol. Scand.* 152:115–124.

Kozlov AM, Darriba D, Flouri T, Morel B, Stamatakis A. 2019. RAxML-NG: a fast, scalable and user-friendly tool for maximum likelihood phylogenetic inference. *Bioinformatics* 35:4453–4455.

Lawrence JP, Rojas B, Fouquet A, Mappes J, Blanchette A, Saporito RA, Bosque RJ, Courtois EA, Noonan BP. 2019. Weak warning signals can persist in the absence of gene flow. *Proc. Natl. Acad. Sci. U. S. A.* 116:19037–19045.

Li D, Liu C-M, Luo R, Sadakane K, Lam T-W. 2015. MEGAHIT: an ultra-fast single-node solution for large and complex metagenomics assembly via succinct de Bruijn graph. *Bioinformatics* 31:1674–1676.

Li H, Durbin R. 2009. Fast and accurate short read alignment with Burrows–Wheeler transform. *Bioinformatics* 25:1754–1760.

Li W, Godzik A. 2006. Cd-hit: a fast program for clustering and comparing large sets of protein or nucleotide sequences. *Bioinformatics* 22:1658–1659.

Liebman PA, Entine G. 1968. Visual pigments of frog and tadpole (*Rana pipiens*). *Vision Res.* 8:761–775.

Maan ME, Cummings ME. 2008. Female preferences for aposematic signal components in a polymorphic poison frog. *Evolution* 62:2334–2345.

Maan ME, Cummings ME. 2009. Sexual dimorphism and directional sexual selection on aposematic signals in a poison frog. *Proc. Natl. Acad. Sci. U. S. A.* 106:19072–19077.

Maan ME, Cummings ME. 2012. Poison frog colors are honest signals of toxicity, particularly for bird predators. *Am. Nat.* 179:E1–E14.

Mappes J, Marples NM, Endler JA. 2005. The complex business of survival by aposematism. *Trends Ecol. Evol.* 20:598–603.

McCulloch KJ, Osorio D, Briscoe AD. 2016. Sexual dimorphism in the compound eye of *Heliconius erato*: a nymphalid butterfly with at least five spectral classes of photoreceptor. *J. Exp. Biol.* 219:2377–2387.

Medina I, Wang IJ, Salazar C, Amézquita A. 2013. Hybridization promotes color polymorphism in the aposematic harlequin poison frog, *Oophaga histrionica*. *Ecol. Evol.* 3:4388–4400.

Melin AD, Fedigan LM, Hiramatsu C, Hiwatashi T, Parr N, Kawamura S. 2009. Fig foraging by dichromatic and trichromatic *Cebus capucinus* in a tropical dry forest. *Int. J. Primatol.* 30:753–775.

Minh BQ, Schmidt HA, Chernomor O, Schrempf D, Woodhams MD, von Haeseler A, Lanfear R. 2020. IQ-TREE 2: New Models and Efficient Methods for Phylogenetic Inference in the Genomic Era. *Mol. Biol. Evol.* 37:1530–1534.

Miyazaki T, Kondrashev SL, Kasagi S, Mizusawa K, Takahashi A. 2017. Sequence and localization of an ultraviolet (*sws1*) opsin in the retina of the Japanese sardine *Sardinops melanostictus* (Teleostei: Clupeiformes). *J. Fish Biol.* 90:954–967.

Mohun SM, Davies WIL. 2019. The evolution of amphibian photoreception. *Front. Ecol. Evol* 7:321.

Murrell B, Wertheim JO, Moola S, Weighill T, Scheffler K, Kosakovsky Pond SL. 2012. Detecting individual sites subject to episodic diversifying selection. *PLoS Genet.* 8:e1002764.

Nathans J, Thomas D, Hogness DS. 1986. Molecular genetics of human color vision: The genes encoding blue, green, and red pigments. *Science* 232:196–202.

Neitz M, Neitz J, Jacobs GH. 1991. Spectral tuning of pigments underlying red-green color vision. *Science* 252:971–974.

Nguyen NTT, Vincens P, Roest Crollius H, Louis A. 2018. Genomicus 2018: Karyotype evolutionary trees and on-the-fly synteny computing. *Nucleic Acids Res.* 46:D816–D822.

Okano T, Kojima D, Fukada Y, Shichida Y, Yoshizawa T. 1992. Primary structures of chicken cone visual pigments: Vertebrate rhodopsins have evolved out of cone visual pigments. *Proc. Natl. Acad. Sci. U. S. A.* 89:5932–5936.

Osorio D, Vorobyev M. 2008. A review of the evolution of animal colour vision and visual communication signals. *Vision Res.* 48:2042–2051.

Palczewski K, Kumasaka T, Hori T, Behnke CA, Motoshima H, Fox BA, Le Trong I, Teller DC, Okada T, Stenkamp RE, et al. 2000. Crystal structure of rhodopsin: A G protein-coupled receptor. *Science* 289:739–745.

Paradis E, Schliep K. 2019. ape 5.0: an environment for modern phylogenetics and evolutionary analyses in R. *Bioinformatics* 35:526–528.

Phillips GAC, Carleton KL, Marshall NJ. 2015. Multiple genetic mechanisms contribute to visual sensitivity variation in the Labridae. *Mol. Biol. Evol.* 33:201–215.

Pombal JP, Sazima I, Célio F. B. Haddad. 1994. Breeding behavior of the Pumpkin Toadlet, *Brachycephalus ephippium* (Brachycephalidae). *J. Herpetol.* 28:516–519.

Pyron RA. 2014. Biogeographic analysis reveals ancient continental vicariance and recent oceanic dispersal in amphibians. *Syst. Biol.* 63:779–797.

Rebouças R, Carollo AB, Freitas MDO, Lambertini C, Dos Santos RMN, Toledo LF. 2019. Is the conspicuous dorsal coloration of the Atlantic forest pumpkin toadlets aposematic? *Salamandra* 55:39–47.

Reynolds RG, Fitzpatrick BM. 2007. Assortative mating in poison-dart frogs based on an ecologically important trait. *Evolution* 61:2253–2259.

Richards-Zawacki CL, Cummings ME. 2011. Intraspecific reproductive character displacement in a polymorphic poison dart frog, *Dendrobates pumilio*. *Evolution* 65:259–267.

Rodríguez A, Mundy NI, Ibáñez R, Pröhl H. 2020. Being red, blue and green: the genetic basis of coloration differences in the strawberry poison frog (*Oophaga pumilio*). *BMC Genomics* 21:301.

Rogers RL, Zhou L, Chu C, Márquez R, Corl A, Linderoth T, Freeborn L, MacManes MD, Xiong Z, Zheng J, et al. 2018. Genomic takeover by transposable elements in the strawberry poison frog. *Mol. Biol. Evol.* 35:2913–2927.

Rohland N, Reich D. 2012. Cost-effective, high-throughput DNA sequencing libraries for multiplexed target capture. *Genome Res.* 22:939–946.

Rojas B, Burdfield-Steel E, De Pasqual C, Gordon S, Hernández L, Mappes J, Nokelainen O, Rönkä K, Lindstedt C. 2018. Multimodal aposematic signals and their emerging role in mate attraction. *Front. Ecol. Evol* 6:93.

Rojas B, Devillechabrolle J, Endler JA. 2014. Paradox lost: Variable colour-pattern geometry is associated with differences in movement in aposematic frogs. *Biol. Lett.* 10:20140193.

Rößler DC, Lötters S, Mappes J, Valkonen JK, Menin M, Lima AP, Pröhl H. 2019. Sole coloration as an unusual aposematic signal in a Neotropical toad. *Sci. Rep.* 9:1128.

Santos JC, Cannatella DC. 2011. Phenotypic integration emerges from aposematism and scale in poison frogs. *Proc. Natl. Acad. Sci. U. S. A.* 108:6175–6180.

Santos JC, Coloma LA, Cannatella DC. 2003. Multiple, recurring origins of aposematism and diet specialization in poison frogs. *Proc. Natl. Acad. Sci. U. S. A.* 100:12792–12797.

Santos JC, Tarvin RD, O'Connell LA, Blackburn DC, Coloma LA. 2018. Diversity within diversity: Parasite species richness in poison frogs assessed by transcriptomics. *Mol. Phylogenet. Evol.* 125:40–50.

Schott RK, Müller J, Yang CGY, Bhattacharyya N, Chan N, Xu M, Morrow JM, Ghenu AH, Loew ER, Tropepe V, et al. 2016. Evolutionary transformation of rod photoreceptors in the all-cone retina of a diurnal garter snake. *Proc. Natl. Acad. Sci. U. S. A.* 113:356–361.

Schott RK, Perez L, Kwiatkowski MA, Imhoff V, Gumm JM. 2022. Evolutionary analyses of visual opsin genes in frogs and toads: Diversity, duplication, and positive selection. *Ecol. Evol.* 12:e8595.

Sherratt TN. 2008. The evolution of Müllerian mimicry. *Naturwissenschaften* 95:681–695.

Siddiqi A, Cronin TW, Loew ER, Vorobyev M, Summers K. 2004. Interspecific and intraspecific views of color signals in the strawberry poison frog *Dendrobates pumilio*. *J. Exp. Biol.* 207:2471–2485.

Stebbins RC, Cohen NW. 1997. A Natural History of Amphibians. Princeton University Press.

Stuckert AMM, Chouteau M, McClure M, LaPolice TM, Linderoth T, Nielsen R, Summers K, MacManes MD. 2021. The genomics of mimicry: Gene expression throughout development provides insights into convergent and divergent phenotypes in a Müllerian mimicry system. *Mol. Ecol.* 30:4039–4061.

Summers K, Symula R, Clough M, Cronin T. 1999. Visual mate choice in poison frogs. *Proc. Biol. Sci.* 266:2141–2145.

Tarvin RD, Powell EA, Santos JC, Ron SR, Cannatella DC. 2017. The birth of aposematism: high phenotypic divergence and low genetic diversity in a young clade of poison frogs. *Mol. Phylogenet. Evol.* 109:283–295.

Thomas KN, Gower DJ, Streicher JW, Bell RC, Fujita MK, Schott RK, Liedtke HC, Haddad CFB, Becker CG, Cox CL, et al. 2022. Ecology drives patterns of spectral transmission in the ocular lenses of frogs and salamanders. *Funct. Ecol.* 36:850–864.

Toledo LF, Haddad CFB. 2009. Colors and some morphological traits as defensive mechanisms in anurans. *Int. J. Zool.* 2009:910892.

Toomey MB, Corbo JC. 2017. Evolution, Development and Function of Vertebrate Cone Oil Droplets.

Front. Neural Circuits 11:97.

Wang IJ. 2011. Inversely related aposematic traits: reduced conspicuousness evolves with increased toxicity in a polymorphic poison-dart frog. *Evolution* 65:1637–1649.

Warrant EJ, Johnsen S. 2013. Vision and the light environment. *Curr. Biol.* 23:R990–R994.

Wells DK. 2007. The ecology & behavior of amphibians. Chicago: University of Chicago Press.

Wollenberg KC, Lötters S, Mora-Ferrer C, Veith M. 2008. Disentangling composite colour patterns in a poison frog species. *Biol. J. Linn. Soc. Lond.* 93:433–444.

Womack MC, Steigerwald E, Blackburn D, Cannatella DC, Catenazzi A, Che J, Koo MS, McGuire JA, Ron SR, Spencer C, et al. 2022. State of the Amphibia 2020: A review of five years of amphibian research and existing resources. *Ichthyology & Herpetology*:in press.

Xu Y, Lei Y, Su Z, Zhao M, Zhang J, Shen G, Wang L, Li J, Qi J, Wu J. 2021. A chromosome-scale Gastrodia elata genome and large-scale comparative genomic analysis indicate convergent evolution by gene loss in mycoheterotrophic and parasitic plants. *Plant J.* 108:1609–1623.

Yang Y, Dugas MB, Sudekum HJ, Murphy SN, Richards-Zawacki CL. 2018. Male-male aggression is unlikely to stabilize a poison frog polymorphism. *J. Evol. Biol.* 31:457–468.

Yang Y, Richards-Zawacki CL. 2020. Male–male contest limits the expression of assortative mate preferences in a polymorphic poison frog. *Behav. Ecol.* 32:151–158.

Yang Y, Richards-Zawacki CL, Devar A, Dugas MB. 2016. Poison frog color morphs express assortative mate preferences in allopatry but not sympatry. *Evolution* 70:2778–2788.

Yang Y, Servedio MR, Richards-Zawacki CL. 2019. Imprinting sets the stage for speciation. *Nature* 574:99–102.

Yeager J, Barnett JB. 2021. The influence of ultraviolet reflectance differs between conspicuous aposematic signals in neotropical butterflies and poison frogs. *Ecol. Evol.* 11:13633–13640.

Yokoyama R, Yokoyama S. 1990. Convergent evolution of the red- and green-like visual pigment genes in fish, Astyanax fasciatus, and human. *Proc. Natl. Acad. Sci. U. S. A.* 87:9315–9318.

Yokoyama S. 2008. Evolution of dim-light and color vision pigments. *Annual Review of Genomics and Human Genetics* 9:259–282.

Yokoyama S, Radlwimmer FB. 1998. The “five-sites” rule and the evolution of red and green color vision in mammals. *Mol. Biol. Evol.* 15:560–567.

Yokoyama S, Radlwimmer FB. 2001. The molecular genetics and evolution of red and green color vision in vertebrates. *Genetics* 158:1697–1710.

Yokoyama S, Starmer WT, Takahashi Y, Tada T. 2006. Tertiary structure and spectral tuning of UV and violet pigments in vertebrates. *Gene* 365:95–103.

Yokoyama S, Tada T. 2003. The spectral tuning in the short wavelength-sensitive type 2 pigments. *Gene* 306:91–98.

Yovanovich CAM, Koskela SM, Nevala N, Kondrashev SL, Kelber A, Donner K. 2017. The dual rod

system of amphibians supports colour discrimination at the absolute visual threshold. *Philos. Trans. R. Soc. Lond. B Biol. Sci.* 372:20160066.

Yovanovich CAM, Pierotti MER, Kelber A, Jorgewich-Cohen G, Ibáñez R, Grant T. 2020. Lens transmittance shapes ultraviolet sensitivity in the eyes of frogs from diverse ecological and phylogenetic backgrounds. *Proc. Biol. Sci.* 287:20192253.

ORDER OF FIGURES ATTACHED TO THIS DOCUMENT (COMPLETE LEGENDS ARE PROVIDED IN-TEXT AND IN THE SUPPLEMENTARY MATERIAL DOCUMENT):

1. **Figure 1**. A summary of color and activity trait data used in analyses (see Table S1 for references) and results from HyPhy selection analyses of two opsin genes, *LWS* and *RH1*.
2. **Figure 2**. A) *SWS2* is found in a syntenic block with *LWS* in the ancestors of all tetrapods (block 355) and in the ancestor of all amniotes (block 65). B) Comparison of *LWS* syntenic block among anuran species.
3. **Figure S1**. A summary of color and activity trait data used in analyses (see Table S1 for references) and results from HyPhy selection analyses of two opsin genes, *SWS1* and *SWS2*.
4. **Figure S2.** Summary of results from Hyphy selection tests.

POSITIVE OR NEGATIVE SELECTION AT SPECIFIC SITES (FEL)

TRAIT LEGEND

- ■ **Coloration:** Bright **Activity:** Diurnal
- □ **Coloration:** Cryptic **Activity:** Nocturnal
- ◘ **Coloration:** Intermediate

BRANCH LEGEND

- Background
- Diurnal (D)
- Diurnal+ Bright coloration (DC)

LWS

RH1

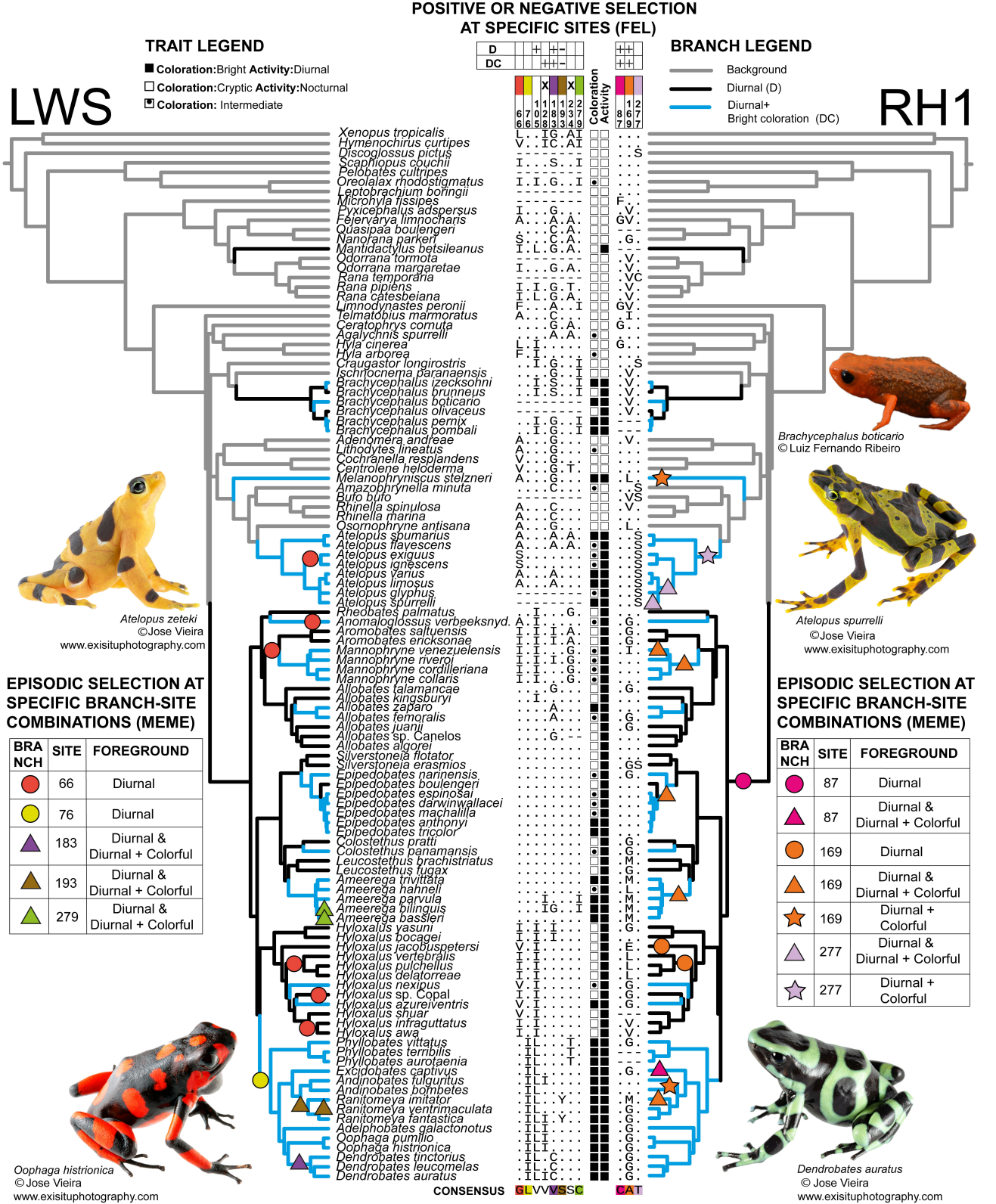

Atelopus zeteki
©Jose Vieira
www.exisituphotography.com

Brachycephalus boticario
© Luiz Fernando Ribeiro

Atelopus spurrelli
©Jose Vieira
www.exisituphotography.com

EPISODIC SELECTION AT SPECIFIC BRANCH-SITE COMBINATIONS (MEME)

BRANCH	SITE	FOREGROUND
●	66	Diurnal
●	76	Diurnal
▲	183	Diurnal & Diurnal + Colorful
▲	193	Diurnal & Diurnal + Colorful
▲	279	Diurnal & Diurnal + Colorful

EPISODIC SELECTION AT SPECIFIC BRANCH-SITE COMBINATIONS (MEME)

BRANCH	SITE	FOREGROUND
●	87	Diurnal
▲	87	Diurnal & Diurnal + Colorful
●	169	Diurnal
▲	169	Diurnal & Diurnal + Colorful
★	169	Diurnal + Colorful
▲	277	Diurnal & Diurnal + Colorful
★	277	Diurnal + Colorful

Oophaga histrionica
© Jose Vieira
www.exisituphotography.com

Dendrobates auratus
© Jose Vieira
www.exisituphotography.com

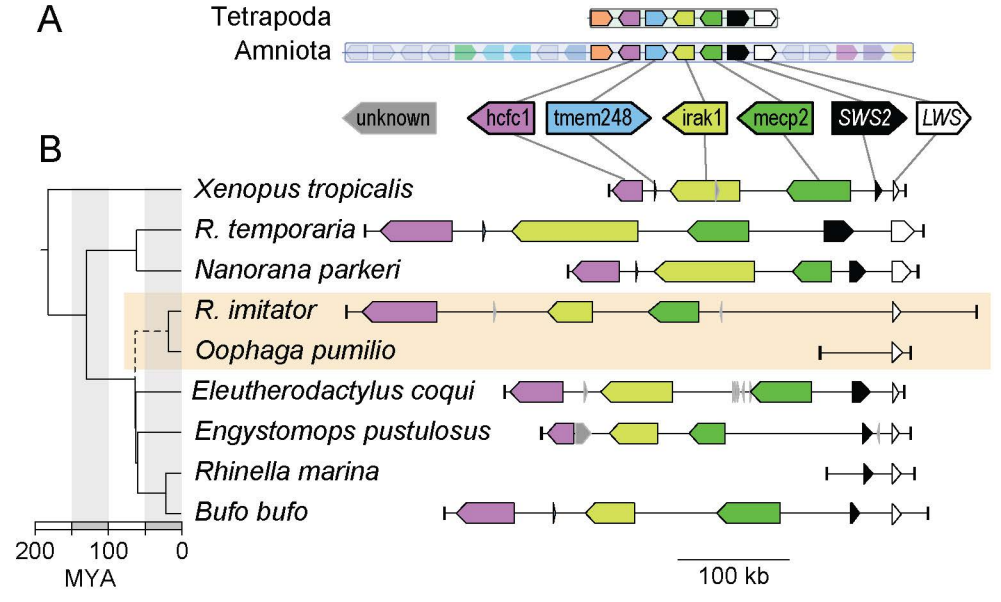
A
Tetrapoda
Amniota
unknown
hcfc1
tmem248
irak1
mecp2
SWS2
LWS
B
Xenopus tropicalis
R. temporaria
Nanorana parkeri
R. imitator
Oophaga pumilio
Eleutherodactylus coqui
Engystomops pustulosus
Rhinella marina
Bufo bufo
200
100
0
MYA
100 kb

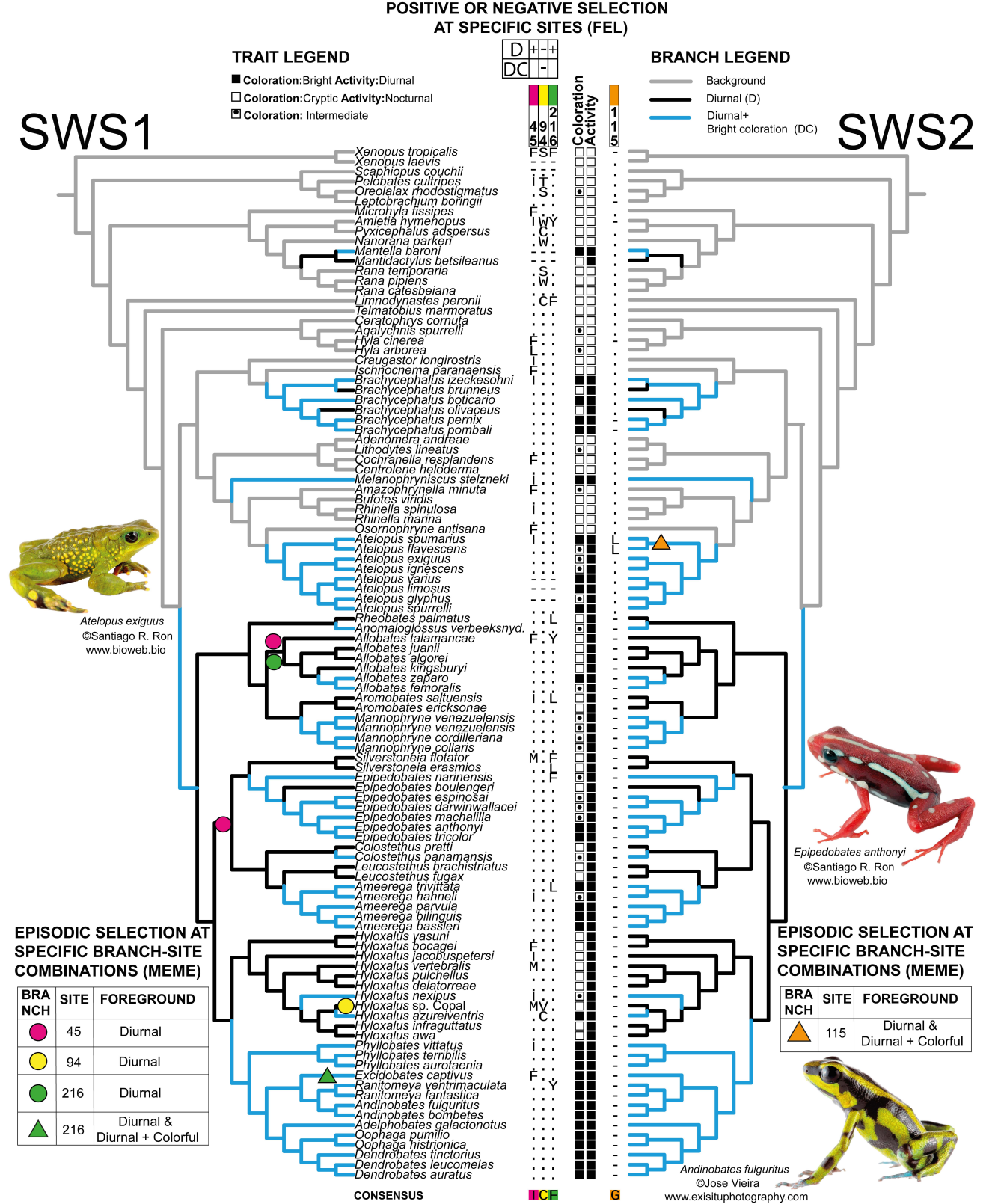
POSITIVE OR NEGATIVE SELECTION
AT SPECIFIC SITES (FEL)
D + - +
DC - -
TRAIT LEGEND
Coloration:Bright Activity:Diurnal
Coloration:Cryptic Activity:Nocturnal
Coloration: Intermediate
BRANCH LEGEND
Background
Diurnal (D)
Diurnal+
Bright coloration (DC)
SWS1
SWS2
Coloration
Activity
Xenopus tropicalis
Xenopus laevis
Scaphiopus couchii
Pelobates cultripes
Oreolalax rhodostigmatus
Leptobrachium boringii
Microhyla fissipes
Amietia hymenopus
Pyxicephalus adspersus
Nanorana parkeri
Mantella baroni
Mantidactylus betsileanus
Rana temporaria
Rana pipiens
Rana catesbeiana
Limnodynastes peronii
Telmatobius marmoratus
Ceratophrys cornuta
Agalychnis spurrelli
Hyla cinerea
Hyla arborea
Craugastor longirostris
Ischnocnema paranaensis
Brachycephalus izeckesohni
Brachycephalus brunneus
Brachycephalus boticario
Brachycephalus olivaceus
Brachycephalus pernix
Brachycephalus pombali
Adenomera andreae
Lithodytes lineatus
Cochranella resplandens
Centrolene heloderma
Melanophryniscus stelzneki
Amazophrynella minuta
Bufotes viridis
Rhinella spinulosa
Rhinella marina
Osornophryne antisana
Atelopus spumarius
Atelopus flavescens
Atelopus exiguus
Atelopus ignescens
Atelopus varius
Atelopus limosus
Atelopus glyphus
Atelopus spurrelli
Rheobates palmatus
Anomaloglossus verbeeksnyd.
Allobates talamancae
Allobates juanii
Allobates algorei
Allobates kingsburyi
Allobates zaparo
Allobates femoralis
Aromobates saltuensis
Aromobates ericksonae
Mannophryne venezuelensis
Mannophryne venezuelensis
Mannophryne cordilleriana
Mannophryne collaris
Silverstoneia flotator
Silverstoneia erasmios
Epipedobates narinensis
Epipedobates boulengeri
Epipedobates espinosai
Epipedobates darwinwallacei
Epipedobates machalilla
Epipedobates anthonyi
Epipedobates tricolor
Colostethus pratti
Colostethus panamansis
Leucostethus brachistriatus
Leucostethus fugax
Ameerega trivittata
Ameerega hahneli
Ameerega parvula
Ameerega bilinguis
Ameerega bassleri
Hyloxalus yasuni
Hyloxalus bocagei
Hyloxalus jacobuspetersi
Hyloxalus vertebralis
Hyloxalus pulchellus
Hyloxalus delatorreae
Hyloxalus nexipus
Hyloxalus sp. Copal
Hyloxalus azureiventris
Hyloxalus infraguttatus
Hyloxalus awa
Phyllobates vittatus
Phyllobates terribilis
Phyllobates aurotaenia
Excidobates captivus
Ranitomeya ventrimaculata
Ranitomeya fantastica
Andinobates fulguritus
Andinobates bombetes
Adelphobates galactonotus
Oophaga pumilio
Oophaga histrionica
Dendrobates tinctorius
Dendrobates leucomelas
Dendrobates auratus
CONSENSUS
Atelopus exiguus
©Santiago R. Ron
www.bioweb.bio
Epipedobates anthonyi
©Santiago R. Ron
www.bioweb.bio
Andinobates fulguritus
©Jose Vieira
www.exisituphotography.com
EPISODIC SELECTION AT SPECIFIC BRANCH-SITE COMBINATIONS (MEME)
BRANCH SITE FOREGROUND
45 Diurnal
94 Diurnal
216 Diurnal
216 Diurnal & Diurnal + Colorful
EPISODIC SELECTION AT SPECIFIC BRANCH-SITE COMBINATIONS (MEME)
BRANCH SITE FOREGROUND
115 Diurnal & Diurnal + Colorful

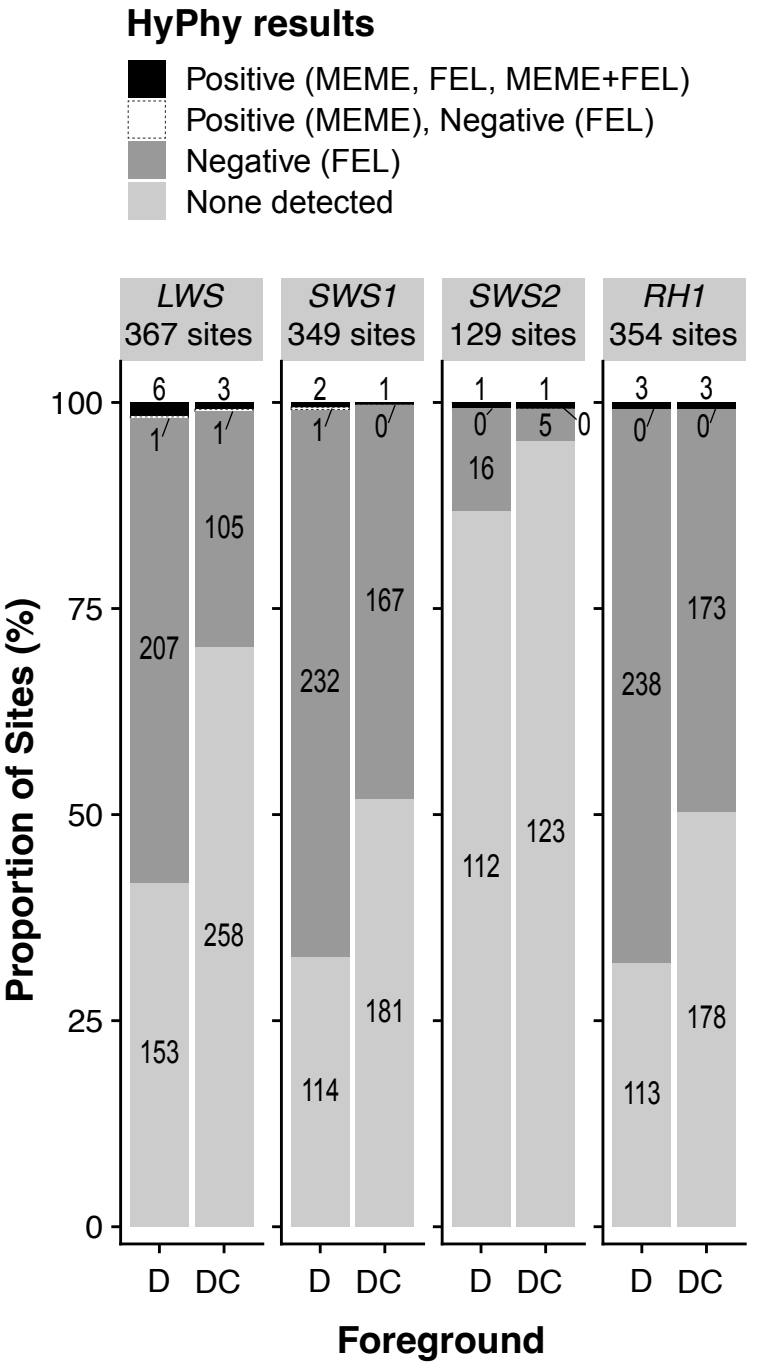
HyPhy results
Positive (MEME, FEL, MEME+FEL)
Positive (MEME), Negative (FEL)
Negative (FEL)
None detected
LWS
367 sites
SWS1
349 sites
SWS2
129 sites
RH1
354 sites
Proportion of Sites (%)
100
75
50
25
0
6
3
1
1
207
105
153
258
2
1
1
0
232
167
114
181
1
1
0
5
0
16
112
123
3
3
0
0
238
173
113
178
D
DC
Foreground